Nebraska Transportation Center

MID-AMERICA TRANSPORTATION CENTER

NDOR Nebraska Department of Roads

Report SPR-P1(15) M016

Final Report
26-1121-4021-001

Research on High-RAP Asphalt Mixtures with Rejuvenators and WMA Additives

Hamzeh Haghshenas
Graduate Research Assistant
Department of Civil Engineering
University of Nebraska-Lincoln

Hesamaddin Nabizadeh
Graduate Research Assistant

Yong-Rak Kim, Ph.D.
Professor

Kommidi Santosh
Graduate Research Assistant

2016

Nebraska Transportation Center
262 WHIT
2200 Vine Street
Lincoln, NE 68583-0851
(402) 472-1975

"This report was funded in part through grant[s] from the Federal Highway Administration [and Federal Transit Administration], U.S. Department of Transportation. The views and opinions of the authors [or agency] expressed herein do not necessarily state or reflect those of the U.S. Department of Transportation."

Research on High-RAP Asphalt Mixtures with Rejuvenators and WMA Additives

Hamzeh Haghshenas
Graduate Research Assistant
Department of Civil Engineering
University of Nebraska-Lincoln

Hesamaddin Nabizadeh
Graduate Research Assistant
Department of Civil Engineering
University of Nebraska-Lincoln

Yong-Rak Kim, Ph.D.
Professor
Department of Civil Engineering
University of Nebraska-Lincoln

Kommidi Santosh
Graduate Research Assistant
Department of Civil Engineering
University of Nebraska-Lincoln

A Report on Research Sponsored by

Nebraska Department of Roads

September 2016

Technical Report Documentation Page

1. Report No SPR-P1(15) M016	2. Government Accession No.	3. Recipient's Catalog No.	
4. Title and Subtitle Research on High-RAP Asphalt Mixtures with Rejuvenators and WMA Additives		5. Report Date September 27, 2016	
		6. Performing Organization Code	
7. Author/s H.F. Haghshenas, H. Nabizadeh, Y-R. Kim, K. Santosh		8. Performing Organization Report No. 26-1121-4021-001	
9. Performing Organization Name and Address University of Nebraska-Lincoln, Department of Civil Engineering 362M Whittier Research Center, Lincoln, NE 68583-0856		10. Work Unit No. (TRAIS)	
		11. Contract or Grant No.	
12. Sponsoring Organization Name and Address Nebraska Department of Roads 1400 Highway 2, PO Box 94759, Lincoln, NE 68509		13. Type of Report and Period Covered	
		14. Sponsoring Agency Code MATC TRB RiP No. 36232	
15. Supplementary Notes			

16. Abstract

This study is to evaluate the mechanical and chemical properties of the asphalt concrete (AC) mixture, fine aggregate matrix (FAM), and binder modified by three different rejuvenators and warm mix asphalt (WMA) additive. In this regard, for testing of AC mixtures, the dynamic modulus, dynamic creep, and semicircular bending (SCB) fracture tests were conducted. For testing of FAM mixtures, three types of strain-controlled torsional oscillatory shear tests (i.e., strain sweep, frequency sweep, and time sweep) and the static creep-recovery tests were employed for comparative purposes. For binders, the Fourier transform infrared (FTIR) spectroscopy, saturates-aromatics-resins-asphaltenes (SARA) analysis, dynamic shear rheometer (DSR), and atomic force microscopy (AFM) were used to characterize the physicochemical and mechanical aspects of the asphalt binders. Based on test and analysis results, the rejuvenators can soften the materials, increase the rutting potential and may mitigate moisture damage resistance, while improving cracking and fatigue resistance of the asphaltic mixtures. A comparison between AC mixtures and corresponding FAM mixtures revealed the interrelationships between the two length scales. From the binder tests, it appears that the rejuvenators decrease either carbonyl or sulfoxide or both indices. Addition of rejuvenators to the mixture of recycled asphalt binder and virgin binder led to a decrease in the amount of asphaltenes. Furthermore, rejuvenators improved colloidal instability index (CII), which implies that the aged binder has become more stable due to rejuvenation. The AFM phase images of binders indicated that the softening effect of rejuvenators corresponds to the mechanical test results from DSR.

17. Key Words	18. Distribution Statement		
19. Security Classification (of this report) Unclassified	20. Security Classification (of this page) Unclassified	21. No. of Pages 66	22. Price

Form DOT F 1700.7 (8-72) Reproduction of form and completed page is authorized

Table of Contents

List of Figures

List of Tables

Disclaimer

This report was funded in part through grant[s] from the Federal Highway Administration [and Federal Transit Administration], U.S. Department of Transportation. The views and opinions of the authors [or agency] expressed herein do not necessarily state or reflect those of the U. S. Department of Transportation.

Acknowledgements

The authors thank the Nebraska Department of Roads (NDOR) for the financial support needed to complete this study. In particular, the authors thank NDOR Technical Advisory Committee (TAC) for their technical support and invaluable discussions/comments.

Chapter 1 Introduction

The expanded use of reclaimed asphalt pavement (RAP) materials in the production of asphalt mixtures has significant economic benefits and environmental advantages through the reduction of material costs and impacts associated with extraction, transportation, and processing of the conventional asphalt materials. Currently, the state of Nebraska allows the usage of RAP up to 40-55% for the production of their asphalt mixtures. Although the higher level of RAP materials in the asphalt mixtures is favorable, there is a major concern that needs further consideration; RAP brings some unwanted properties in the asphalt mixture such as aged binder with high stiffness and possibly some partially binder-coated aggregates. In order to mitigate the problems related to RAP, many efforts have been carried out with different approaches (Carpenter and Wolosick, 1980; Hajj et al., 2011; Hoppe et al., 2015; Huang et al., 2011; Mogawer et al., 2013; Sengoz and Oylumluoglu, 2013; Shu et al., 2008; Stimilli et al., 2015; Tran et al., 2012; Zaumanis et al., 2013; Zhou et al., 2014).

The most critical obstacle in using high-RAP asphalt mixtures is the high stiffness observed in such mixtures, which results in low workability. The inadequate workability of the asphalt mixtures prevents proper compaction in the field and can ultimately lead to premature field failure (Mogawer et al., 2012). Recently, rejuvenators and soft binders have been introduced as modifying agents that can effectively improve the engineering properties of the asphalt mixtures that contain a high content of RAP. For instance, a rejuvenator contains a high proportion of maltenes (mostly small molecular weights of condensed aromatics hydrocarbons called resins). Actually, a rejuvenator re-balanced the composition of the aged binder, which lost its maltenes during construction and service (Tran et al., 2012). In this way, the rejuvenator can decrease the stiffness of the oxidized asphalt mixtures.

The effect of rejuvenators on the mechanical properties and performance of the mixtures or binders has been extensively studied (Hajj et al., 2013; Hill et al., 2013; Im and Zhou, 2014; Zaumanis et al., 2013). Shen et al. (2007) reported that the rejuvenator content of the asphalt mixtures significantly affects the properties of aged binders and mixtures. Similarly, Mogawer et al. (2013) have shown that the rejuvenators can mitigate the stiffness of the binder and improve the cracking resistance of the mixtures. In addition to the role of rejuvenators, warm mix asphalt (WMA) technology shows a great potential to be incorporated with the high-RAP asphalt mixtures because WMA additives can also improve workability by reducing the viscosity of the mixtures. Among various WMA technologies, amine-based products (such as Evotherm) can also contribute to moisture damage resistance when they are associated with anti-strip agents. This is particularly desired for Nebraska because the amine-based WMA additive can potentially replace (or at least partially supplement) hydrated lime, which is imported from other states. Historically, hydrated lime has been added to typical Nebraska asphalt mixtures to mitigate moisture damage potential.

Incorporation of the rejuvenators and WMA additives in the high-RAP asphalt provides economical, technical, and environmental benefits; however, the effects on mixture properties and long-term performance leave many questions remaining. This research is therefore to investigate the effects of rejuvenators and WMA additives on high-RAP mixture properties and performance characteristics. The results of this research are expected to bring significant outcomes to maximize

the use of RAP in Nebraska without compromising core engineering properties for long-term pavement performance. Currently Nebraska allows up to 55% RAP in some of its mixtures with a state average RAP content of nearly 40%. This research is focusing on rejuvenators and its effects for Nebraska to utilize mixture with 65% RAP contents and still provide engineered designs that provide quality and pavement performance.

1.1 Research Objectives and Scope

This research evaluated the properties and characteristics of asphaltic materials in three different scales (i.e., asphalt concrete (AC), fine aggregate matrix (FAM), and asphalt binder). FAM is composed of asphalt binder and fine aggregates passing the No.16 sieve. Binders are blended with aged materials from the RAP, three different rejuvenators, and the WMA additive (Evotherm). For the testing of AC mixtures, the dynamic modulus, dynamic creep, and semi-circular bending (SCB) fracture tests were conducted. For testing of FAM mixtures, three types of strain-controlled torsional oscillatory shear tests (i.e., strain sweep, frequency sweep, and time sweep) and the static creep-recovery tests were employed for comparative purposes. For binders, the Fourier transform infrared (FTIR) spectroscopy, saturates-aromatics-resins-asphaltenes (SARA) analysis, dynamic shear rheometer (DSR), and atomic force microscopy (AFM) were applied to characterize the physicochemical and mechanical aspects of the asphalt binders.

1.2 Organization of the Report

This report consists of five chapters. Following this introduction, Chapter 2 summarizes the literature review on the RAP, rejuvenators, WMA additives, and performance of mixtures and pavements due to the addition of rejuvenators. In Chapter 3, the material selection and sample fabrication procedures to conduct various laboratory tests are described. Chapter 4 introduces the laboratory tests performed to examine mechanical, physical, and chemical characteristics of AC and FAM mixtures and binders that are mixed with and without aged materials, rejuvenators, and WMA additive. Test results and analyses of test data are also presented and discussed in Chapter 4. Finally, Chapter 5 summarizes the main findings and conclusions of this study.

Chapter 2 Background

Nowadays, the use of reclaimed asphalt pavement (RAP) has grown widely in an effort to reduce the use of virgin materials, environmental friendliness, and economic benefits. In general, RAP is the reprocessed materials containing asphalt and aggregates generated after the removal of asphalt pavements for construction, resurfacing, etc. RAP can be comprised of various quality and graded aggregates coated by asphalt cement. In general, "high-RAP asphalt mixture" is the term given to the mixtures with higher than 25% RAP content.

According to the published statistics, the average percentage of asphalt producer companies that use RAP increased from 96% in 2009 to 100% in 2013. Additionally, the average percentage of RAP content in the asphalt mixtures increased from 16.2% in 2009 to 20.0% in 2013 (Hansen and Copeland, 2014). In addition to the great economic savings and environmental benefits, the use of RAP in asphalt mixtures can generally improve the rutting and moisture resistance of the mixtures. However, it should be noted that a high amount of RAP can also reduce the cracking resistance and durability of asphalt mixtures.

Five common approaches for improving RAP mixtures performance are: 1) simply decreasing the amount of RAP, 2) increasing the design density (or reducing N_{design}), 3) adding soft virgin binders, 4) rejuvenating the RAP binder, and 5) blending RAP with WMA additives. Among these approaches, rejuvenating agents/rejuvenators have received great attention because they can improve the mechanical properties—such as cracking resistance—of the asphalt mixtures with high RAP contents. In addition, not only is the blending of WMA with RAP a very cost-effective approach, but the enhanced workability of WMA can also facilitate the use of a higher amount of RAP. It is worthy to note that the addition of WMA additives decreases the mixing temperatures and can consequently, lower the unfavorable binder aging phenomenon. Finally, the RAP mixture that is produced at warm mixture temperatures has still sufficient stiffness and viscoelasticity against rutting and cracking, respectively (NCAT, 2015).

2.1 Historical Viewpoint

Undoubtedly one of the great successes in the asphalt paving industry is the unmatched use of recycled materials; RAP, shingles, glass, and ground tire rubber. Although the recycling of asphalt pavements dates back to 1915 (Kandhal and Mallick, 1998), the major emphasis on the reuse of this waste material started in the 1970s, when the asphalt binder prices increased (Arab oil embargo) and the milling/grinding/profiling machines improved. An understandable answer to such a situation was the implementation of recycling methods for the effective usage of these waste materials with the aim of cost reduction. The effect of such efforts in the development of recycling methods is that now the RAP materials can be considered as routine materials for pavement construction and rehabilitation (West, 2010).

The environmental advantages of recycling strategies include decreasing the gas/dust emission caused by the extraction and transportation of virgin materials, reducing demands on non-renewable resources, and minimizing the landfill space needed for the disposal of used pavements. These environmental benefits, together with the economic savings related to the lower

consumption of virgin aggregates and binders and their transportation expenses, ensure a very sustainable future of RAP materials. According to Hansen (2013), the asphalt production costs include four major categories: materials, plant production, trucking, and lay down (Figure 2-1), and the cost savings in the materials category far outweighs the other from an economic viewpoint.

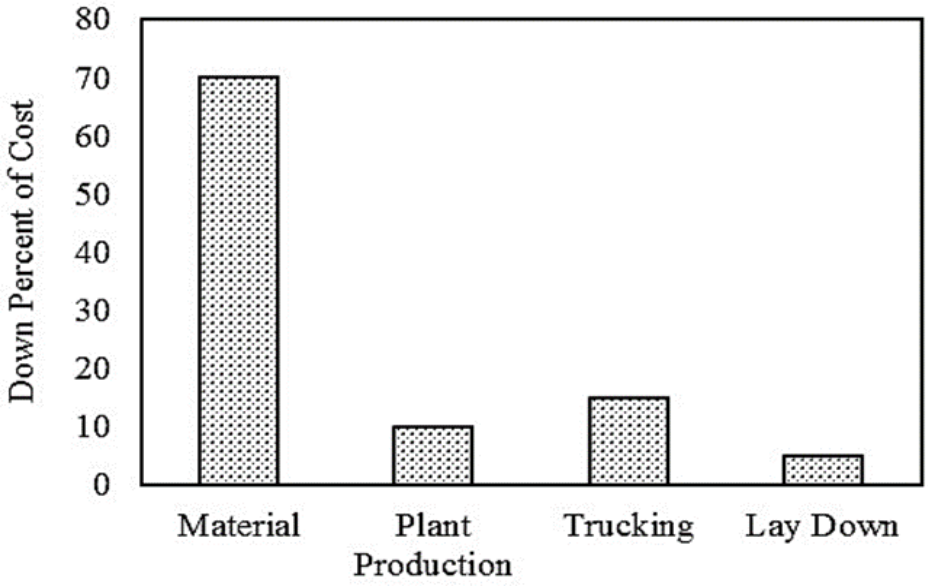

Figure 2-1. The major cost categories in asphalt production (Hansen, 2013).

There was an increase in RAP usage in about half of all states (Copeland 2011) during 2007 to 2009, due to a binder and polymer shortage. Additionally, around half of the state transportation departments reported the performance appraisal of the mixtures with a high RAP content. Although many of the state transportation departments employed higher amounts of RAP in the hot mix asphalt (HMA), the high RAP mixture was not conventional in 2011 (Bonaquist, 2013). Copeland (2011) reported that the most of transportation departments permit the use of more than 25% RAP in HMA layers; however, around half of the States actually use more than 20 percent RAP (Figure 2-2). According to published reports, the average use of RAP in the mixtures reached 100% in 2013, and the average content of RAP in the mixtures increased to 20% by 2013. In addition, 87% of the contractors/branches used excessive amounts of RAP in 2013 (Hansen and Copeland, 2014).

Although there is pessimistic attitude within the pavement community about the use of RAP materials in the new asphalt mixtures, the mixtures with a moderate to high content of RAP should be given much heed. In a recent study, the performance of recycled and virgin mixtures has been compared based on long-term pavement performance (LTPP) data collected from 18 US states and Canadian provinces. It has been ascertained that the performance of the mixtures with at least 30% RAP is similar to that of the virgin mixtures (West et al., 2011). With respect to the economic savings and environmental benefits, it seems that each State's Department of Transportation (DOT) in the US should increase the amount of RAP (even up to 50%) in their flexible pavements. Properly engineering these blends of RAP materials with the other constitutes is one necessary step towards arriving at a desired mixture performance. The effect on asphalt mixtures with a high

RAP content must be designed properly to provide the desired mechanical properties, durability, and performance.

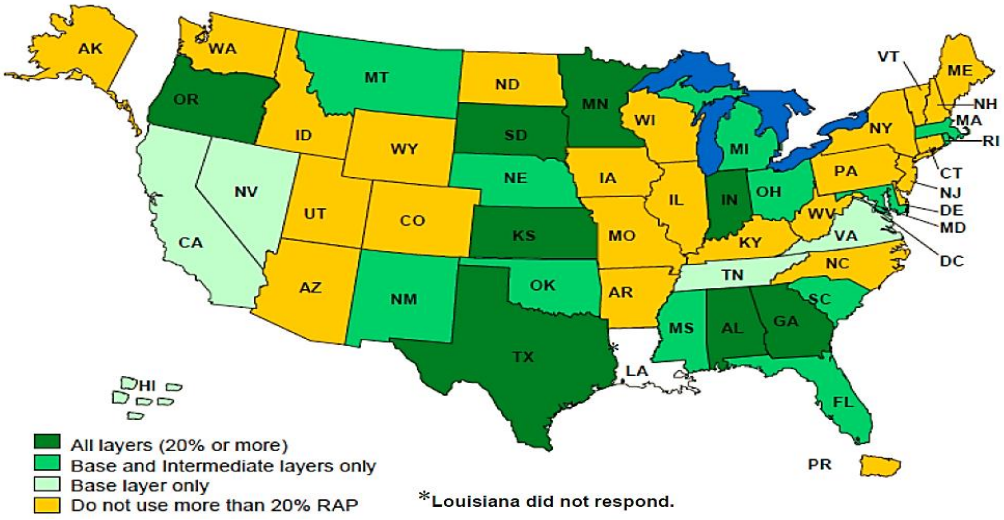

Figure 2-2. States that use more than 20 % RAP in HMA layers (Copeland, 2011).

In the following sections, the effect of RAP materials on the performance of mixtures will be described based on the literature review. Additionally, two common approaches for the improvement of mixture performance are discussed.

2.2 Performance of RAP Mixtures: Stiffness and Resistance to Moisture, Rutting and Cracking

Many studies on RAP mixtures have shown that the addition of RAP in asphalt mixtures changes the mechanical properties. The mechanical changes of the mixture can affect the performance either positively or negatively. In the following section, four major mechanical properties of the mixture containing RAP materials are discussed.

2.2.1 Stiffness

Despite the benefits of RAP, the most common concern is the increase in stiffness of the mixtures, which is due to the aged asphalt binder present in RAP (Al-Qadi et al., 2012; West et al., 2013). This means the fatigue behavior and low-temperature brittleness of the mixtures containing RAP materials are not similar to the mixtures with virgin binder (Daniel et al., 2010; Khosla et al., 2012; McDaniel et al., 2007; Tam et al., 1992).

The most conventional test for the estimation of asphalt mixture stiffness is the dynamic modulus test. Li et al. (2004) showed that by increasing the amount of RAP (0%, 20%, and 40%) in the mixture (Minnesota asphalt mixtures), the dynamic modulus increases. Cross et al. (2007) found that mixtures with 25% RAP have a higher average stiffness than non-RAP mixtures; the value of increase in stiffness was equal to the value of increase in stiffness produced by one level of increasing the PG binder grade. Researchers in Illinois also performed the dynamic modulus test

on 0%, 20%, and 40% RAP mixtures (Al-Qadi et al., 2009). They found that there was a fairly insignificant difference between the dynamic modulus of 0% and 20% RAP mixture. However, the mixture with 40% RAP had a distinctively higher dynamic modulus. The effect of asphalt binder on the stiffness of mixtures containing RAP (0%, 20%, 40% and 100%) was evaluated by Boriack et al. (2014). According to their results, a 0.5% increase in the binder content decreased the dynamic modulus of 0% and 20% RAP mixtures slightly. Additionally, when 1.0% binder was added, the dynamic modulus of 40% RAP mixture decreased. The stiffness of the 100% RAP mixtures was also considerably higher than all other mixtures. On average, the dynamic modulus of the 100% RAP mixtures was 400% and 125% higher than the other mixtures at the lowest and highest loading frequencies, respectively (Boriack and Tomlinson, 2014).

2.2.2 Moisture Resistance

There is no general agreement among researchers regarding moisture resistance of mixtures containing RAP materials. However, it is worthy to note that the RAP aggregates are generally pre-coated with asphalt, which prevents the penetration of moisture into the particles, and consequently, some researchers claim that the mixtures with a high content of RAP are less susceptible to stripping compared to the conventional asphalt mixtures (Tran et al., 2012). Some researchers have reported that the moisture resistance of the asphalt mixtures increases by adding a high amount of RAP (Al-Qadi et al., 2012; Mogawer et al., 2012; Sengoz and Oylumluoglu, 2013). For instance, Tran et al. (2012) have shown that the tensile strength ratio (TSR), as an indicator for predicting moisture susceptibility of different asphalt mixtures with 50% RAP materials, increases approximately 55%. In addition, Ghabchi et al. (2014) have reported that the quality of the asphalt binders coating the different types of aggregates (limestone, rhyolite, sandstone, granite, gravel, and basalt) improves the wettability and reduces the moisture-induced damage potential by increasing the RAP content (0%, 10%, 25%, and 40%). In Table 2-1, the results of different works on the effect of RAP on the moisture sensitivity of different asphalt mixtures are summarized. These results are based on the Modified Lottman test and Hamburg Wheel Track test.

Table 2-1. Effect of RAP on Mixture Resistance to Moisture Damage (Bonaquist, 2013).

Study	Mixture Type	RAP Content	Test Method	
			Tensile Strength Ratio	Hamburg
Gardiner and Wanger (1999)	Lab HMA	0, 15–40	Improves	
Mogawer et al. (2012)	Plant HMA	0–40		No difference
Zhao et al. (2012)	Plant WMA	0, 30, 40, 50	Improves	Improves
	Plant HMA	0, 30	Improves	Improves
Hajj et al. (2011)	Plant and lab HMA	0, 15, 30	No difference	
West et al. (2013)	Lab HMA	0, 25, 40, 55	Mixture dependent	

2.2.3 Rutting Resistance

There is a general agreement among researchers on the positive effect of RAP materials on rutting resistance (Zhou et al., 2011); i.e., rutting resistance improves by increasing the RAP content of the mixtures. McDaniel et al. (2000) examined the effects of RAP content (0%, 10%, 20% and 40%) on the stiffness of asphalt mixtures via shear test. They showed that a higher content of RAP results in higher stiffness and lower shear deformation, which is indicative of increased rutting resistance (Al-Qadi et al., 2012; McDaniel et al., 2000). Moreover, Al-Qadi et al. (2012) demonstrated that the rutting potential of different asphalt mixtures containing 50% RAP materials is reduced in accordance with the wheel tracking and flow number tests.

In a unique research program conducted by West et al. (2012), real-world pavement construction with live heavy trafficking was implemented for the rapid testing and analyzing of the asphalt mixtures with 50% RAP content. The findings of this research program revealed that the asphalt mixtures with 50% RAP content have excellent rutting resistance during the test track (West et al., 2012). Furthermore, Mogawer et al. (2012) evaluated plant-produced mixtures with different RAP content (0% to 40%) and various PG binders (PG52-34, PG58-28, PG64-22, and PG64-28) in three states: New York, New Hampshire, and Vermont. In this study, the effect of RAP content and other pertinent parameters (aggregate temperature, discharge temperature, and storage time) on the rutting resistance of the mixtures were evaluated according to AASHTO T324 "Hamburg Wheel-Track Testing of Compacted Hot-Mix Asphalt (HMA)." The obtained results revealed that all the Vermont mixtures had poor rutting performance. The New Hampshire and New York mixtures could pass the rutting test. Table 2-2 shows the results of several works on the effects of RAP on rutting resistance by using a variety of tests.

Table 2-2. Effect of RAP on Mixture Rutting.

Study	Mixture Type	RAP Content	Test				
			Hamburg Wheel-Track	Flow Number	Pavement Test Track	Shear	Asphalt Pavement Analyzer
McDaniel et al. (2000)	Lab HMA	0, 10, 20, 40				Decreases	
Al-Qadi et al. (2012)	Lab HMA	0-50	Decreases	Decreases			
Xiao et al. (2007)	Lab HMA	0, 15, 25, 30, 38					Decreases
Mogawer et al. (2012)	Plant HMA	0-40	Decreases				
West et al. (2012)	Lab WMA	0, 50			Slightly Increase		
	Lab HMA	0, 50			Decreases		

2.2.4 Cracking Resistance

At first glance, one expects that the aged stiff binder present in RAP increases the stiffness of the mixture (Al-Qadi et al., 2012; West et al., 2013) and, accordingly, leads to fatigue failure and low-temperature brittleness (Daniel et al., 2010; McDaniel et al., 2007). Huang et al. (2011) have reported that the presence of RAP materials in HMA mixtures generally decreases the cracking resistance. In addition, McDaniel et al. (2000) showed that the stiffness of mixtures increases more with a higher content of RAP, which can intensify the probability of low temperature cracking. Moreover, West et al. (2013) have shown that the fracture energy, which is an indicator of fatigue cracking, is higher for the virgin mixtures compared to the mixtures with 55% RAP content. However, recently Stimilli et al. (2015) found that with the proper choice of the RAP material and the type and quantity of the virgin binder, the cracking resistance of the mixture can be improved at low temperatures. In Table 2-3, the results of the works on the effect of RAP associated with cracking resistance are presented. Table 2-4 summarizes the findings of different research on the effect of RAP on thermal cracking resistance. As it can be concluded from the research and in Table 2-4, the resistance to thermal cracking generally decreases for mixtures with a RAP content higher than 25%.

Table 2-3. Effect of RAP on Mixture Resistance to Load-Associated Cracking (Bonaquist, 2013).

Study	Mixture Type	RAP Content	Test				
			Flexural Fatigue	Energy Ratio	Overlay Tester	Cyclic Direct Tension	Indirect Tension Fracture Energy
McDaniel et al. (2000)	Lab HMA	0, 10, 20, 40	Decreases				
Shu et al. (2008)	Lab HMA	0, 10, 20, 30	Decreases	Decreases			
Hajj et al. (2009)	Lab HMA	0, 15, 30	Decreases				
Mogawer et al. (2012)	Plant HMA	0-40			Decreases		
Zhao et al. (2012)	Lab WMA	0, 30, 40, 50	Increases	Increases			
	Lab HMA	0, 30	Decreases	Increases			
West et al. (2013)	Lab HMA	0, 25, 40, 55					Decreases
Li and Gibson (2013)	Lab HMA	0, 20, 40				Decreases	

Table 2-4. Effect of RAP on Mixture Resistance to Low-Temperature Cracking (Bonaquist, 2013).

Study	Mixture Type	RAP Content	Low-Temperature Cracking			
			Disc-Shaped Compact Tension	Semicircular Bend	Indirect Tension	Thermal Stress Restrained Specimen Test
Li et al. (2008)	Lab HMA	0, 20,40		Lower fracture energy for 40%		
McDaniel et al. (2012)	Plant HMA	0, 15, 25, and 40			Lower cracking temperature for 40%	
Hajj et al. (2011)	Plant and Lab HMA	0, 15, 50				Higher fracture temperature for 50%
Behnia et al. (2010)	Lab HMA	0, 30	Lower fracture energy for 30%			
West et al. (2013)	Lab HMA	0, 25, 40, 55		Mixture and temperature dependent		

2.3 Strategies to Improve Cracking Resistance

As discussed in the previous section, one major concern in the use of RAP materials in asphalt mixtures is the decrease in the cracking resistance. The cracking resistance has a direct relationship with the durability of the asphalt mixtures. There are five main strategies to overcome this obstacle and restore the cracking resistance of RAP mixtures (Zhou et al., 2014):

- reducing the usage of RAP (or binder replacement amount),
- increasing design density (lowering design air voids) or reducing N_{design},
- using soft virgin binders, especially for the low-temperature grade,
- rejuvenating RAP binder,
- combining RAP materials with WMA.

2.3.1 Rejuvenating Agents

Rejuvenating agents can improve the mechanical properties of the asphalt mixtures with high RAP content. Regarding the severe aging and different chemical composition of RAP (compared to regular asphalt binder), the reconstituting of the chemical composition of RAP binder is essential, to balance stiffening effect. Hence, softening agents and rejuvenators have been conventionally used to moderate the stiffness of the RAP binders. The role of these softening agents is to decrease the viscosity of the aged bitumen. Examples of the softening agents are the asphalt flux oil, lube stock, and slurry oil. Rejuvenating agents, on the other hand, reconstitute the chemical composition of the binders (Shen et al., 2007). They typically consist of a lubricant and extender oil with a high proportion of maltenes. The rejuvenators can restore the asphaltenes/maltenes ratio. The uniform dispersion of rejuvenator within the recycled mixture and its diffusion into the surface of the aggregates are the most important issues in the effectiveness of a rejuvenator. Table 2-5, shows the five major categories of the rejuvenators (NCAT, 2014).

Table 2-5. Types of Rejuvenators (NCAT, 2014).

Category	Examples	Description
Paraffinic Oils	Waste Engine Oil (WEO) Waste Engine Oil Bottoms (WEOB) Valero VP 165® Storbit®	Refined used lubricating oils
Aromatic Extracts	Hydrolene® Reclamite® Cyclogen L® ValAro 130A®	Refined crude oil products with polar aromatic oil components
Naphthenic Oils	SonneWarmix RJ™ Ergon HyPrene®	Engineered hydrocarbons for asphalt modification
Triglycerides & Fatty Acids	Waste Vegetable Oil Waste Vegetable Grease Brown Grease	Derived from vegetable oils, Has other key chemical elements in addition to triglycerides and fatty acids
Tall Oils	Sylvaroad™ RP1000 Hydrogreen®	Paper industry byproducts, Same chemical family as liquid antistrip agents and emulsifiers

The use of rejuvenators potentially improves the cracking resistance of RAP mixtures. However, the effect of rejuvenators on the rutting and moisture susceptibility of RAP mixtures still remains unclear. Mogawer et al. (2013) have reported the improvement in cracking resistance of the asphalt mixture by adding rejuvenators; however, the rutting and moisture susceptibility increase. Similarly, Uzarowsk L et al. (2010) have observed a significant drop in the rutting resistance and stiffness of the mixture when the rejuvenator is added. In contrast, Zaumanis et al. (2013) and Tran et al. (2012) have reported that not only does the cracking resistance of the rejuvenating agents improve, but they can also successfully pass the rutting resistance requirements. In another study,

Zaumanis et al. (2014) have evaluated 100% recycled HMA lab samples, which were modified by one proprietary and five generic rejuvenators. All the samples showed higher rutting resistance, longer fatigue life, and lower critical cracking temperature compared to the virgin mixtures. Additionally, Im and Zhou (2014) have stated that the RAP mixtures shows improved cracking, moisture, and rutting resistance when different rejuvenators are added to the mixtures.

2.3.2 Warm Mix Asphalt

Regarding global warming, air pollution, and fuel efficiency, the replacement of hot mix asphalt (HMA) by warm mix asphalt (WMA) seems essential. The major advantage of WMA is the lower processing temperatures in comparison with HMA due to the lower viscosity of asphalt binder and higher workability of WMA mixture acquired by minimum heat (Chowdhury and Button, 2008). The other advantages of WMA can be summarized as (Kim, 2011):

- less burner fuel required to heat the aggregates,
- lower emissions at the asphalt plant,
- less hardening of the asphalt binder in mixing and placement,
- less worker exposure to fumes and smoke during the placement operation,
- lower compaction temperature in the field,
- longer construction season,
- increased pavement density,
- longer haul distances,
- the ability to incorporate higher percentages of RAP,
- the ability to place and compact thicker lifts, and
- the ability to open to traffic sooner.

In addition to the WMA capability to reduce the binder resistance at high shear forces (useful in mixing and compaction), they keep the resistance to the normal stresses subjected by traffic loading. In 2004, when WMA was introduced in the US, few WMA additives/processes were practically accessible. Nowadays, more than 30 WMA technologies are in wide use. Considering the type of additives used, WMA technologies can be classified as (Zhang, 2010):

- foaming techniques (e.g., synthetic zeolite),
- organic or wax additives (e.g., Sasobit®), and
- chemical additives (e.g., Evotherm®).

The main advantage of the above mentioned technologies is the reduction in the mixing and compaction temperatures from approximately 155 ˚C (conventional HMA mixtures) to a range of 100 – 140 ˚C (Kavussi et al., 2014). However, adhesion failure is the major concern of decreasing the temperature because the moisture may partially remain in the aggregate (Khodaii et al., 2012). Among different WMA technologies, the amine-based compounds, such as Evotherm®, can effectively improve the moisture damage resistance. By implementing Hamburg testing, Kuang (2012) has demonstrated that there is no moisture failure for the mixtures containing Evotherm®. In addition, Hurley and Prowell (2006) reported that the new Evotherm® generation increases the tensile strength, and the visual stripping disappears. It should be noted that the amine-based WMA technology is heavily used in Nebraska because the hydrated lime has been successfully substituted by these amine-based WMA additives.

According to the survey conducted by the North Carolina Department of Transportation (NCDOT), 12 state transportation departments have employed WMA in the mixtures with high RAP contents (Copeland, 2011). Since 2009, at least 14 state transportation departments have adopted the specifications to accommodate the WMA. In Alabama, Florida, Illinois, Kentucky, and Texas, the procedure applied for using RAP in WMA mixtures has been similar to HMA mixtures. However, in Ohio and South Carolina, some modifications have been considered for use in high RAP content asphalt mixtures. In South Carolina, producers use up to 10% of the more fractionated RAP in WMA before changing the binder grade (Copeland, 2011). It should be noted that fractionation is defined as the act of processing and separating RAP into at least two sizes, typically a coarse fraction and a fine fraction. In most states, the use of RAP materials in mixtures produced via WMA technologies is allowed mainly due to the sustainable advantages of WMA/RAP combinations. In addition, the combination of WMA and RAP provide synergistic effects regarding the pavement performance.

A survey of previous literature on the effects of WMA and RAP on the properties of asphalt mixtures provides some valuable clues. For instance, Zaumanis and Smirnovs (2011) found that by lowering the bitumen viscosity in the WMA production process, a higher percentage of RAP materials can be used. They have also reported that there is no significant problem in the compaction process of the asphalt mixtures with even 90% RAP materials. Furthermore, Mogawer et al. (2013) have found that the high amount of RAP (40%) together with WMA can reduce the cracking resistance of the asphalt rubber gap-graded mixtures. Also, the use of RAP and WMA does not negatively impact the moisture susceptibility and rutting of the mixture. Besides, the workability of the mixtures improves by using the WMA, and the use of WMA and rejuvenator can improve the reflective cracking resistance of the mixtures (Mogawer, 2012). In a research project conducted by Penn State, it has been shown that WMA additives (Evotherm® and Sasobit®) yield an even higher TSR compared to HMA when the amount of RAP is limited to 15% (Solaimanian et al., 2011). Additionally, the result of a research study at Clemson University showed that the presence of WMA in the RAP mixtures has no distinctive effect on the indirect tensile strength, and when the RAP content increases, the rut depth of WMA mixtures generally decreases (Putman, 2012).

2.4 Fine Aggregate Matrix (FAM)

An asphalt concrete (AC) mixture is composed of coarse aggregates and a matrix phase, and the matrix phase is considered herein a separate phase containing asphalt binder, fine aggregates passing sieve No. 16 (mesh size of 1.18 mm), and entrained air voids. The matrix phase has been called FAM in numerous research studies (Branco, 2009; Im et al., 2015; Karki, 2010; Karki et al., 2015; Kim and Aragão, 2013; Kim et al., 2002; Kim and Little, 2005; Kim et al., 2003; Kim et al., 2006; Palvadi et al., 2012; Underwood and Kim, 2013; Vasconcelos et al., 2010). A microstructure of asphalt concrete is illustrated in Figure 2-3, and coarse aggregates and FAM phase can easily be seen in the figure.

FAM plays a substantial role on the performance characteristics (e.g., viscoelastic and viscoplastic properties, fatigue resistance) of asphalt mixtures, and the quality of FAM considerably affects the mechanical characteristics of the entire asphalt concrete mixture. Several studies have been conducted to develop a specification-type testing methodology using FAM to predict the behavior

of the entire asphalt mixture (Haghshenas et al., 2016; Im, 2012; Im et al., 2015; Karki, 2010; Karki et al., 2015; Kim and Aragão, 2013; Li et al., 2015; Underwood and Kim, 2012; Underwood and Kim, 2013).

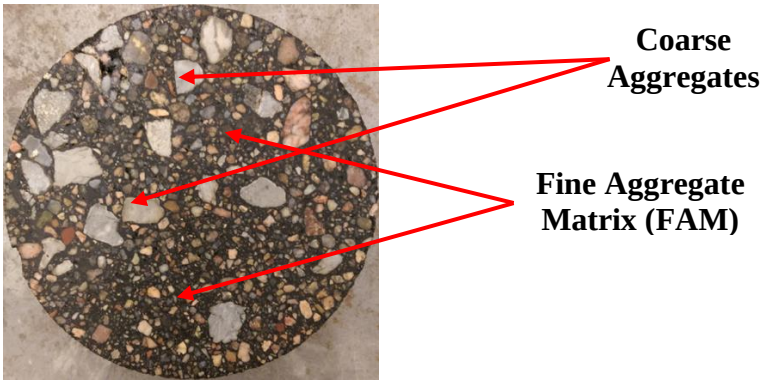

Figure 2-3. Asphalt concrete microstructure with two phases: coarse aggregates and fine aggregate matrix (FAM).

Kim and Little (2005) explored a test to evaluate the effect of fine aggregates and mineral fillers on the fatigue damage. They made small cylindrical sand asphalt samples (12 mm in diameter, 50 mm long) using mastics, pure binders, and modified binders. Different dynamic mechanical tests in a strain-controlled mode (i.e., strain sweep test, frequency sweep test, and time sweep test) were performed using a dynamic mechanical analyzer. They performed frequency sweep tests to determine viscoelastic properties of sand asphalt samples and evaluated fatigue resistance of mixtures by conducting time sweep tests. They found sand asphalt samples could successfully characterize basic material properties and fatigue damage performance of binders and mastics.

Branco (2009) tried to develop a new methodology to evaluate fatigue cracking of the FAM phase of asphalt mixtures using a dynamic mechanical analyzer. To that end, two methods were employed: 1) computing the energy dissipated in viscoelastic deformation, permanent deformation, and fracture, and 2) applying a constitutive relationship to model nonlinear viscoelastic response and damage under cyclic loading. Then, small FAM specimens were fabricated, and different types of torsional shear tests (e.g., strain sweep, time sweep) were performed. Finally, the researcher developed two new methods to evaluate fatigue damage in asphalt mixture independent of the mode of loading.

Vasconcelos et al. (2010) experimentally evaluated the diffusion of water in different FAM mixtures using gravimetric sorption measurement. They regarded FAM as a representative homogenous volume of hot mix asphalt. Two aggregate types (i.e., Basalt and Granite) and three asphalt binders (i.e., PG 58-22, PG 58-28, and PG 58-10) were selected to make FAM specimens; by doing experimental tests, it was inferred that FAM could successfully estimate water diffusion. Karki (2010) used a computational micromechanics model to estimate the dynamic modulus of asphalt concrete mixtures using the properties of the constituents in the heterogeneous microstructure. The model considered the asphalt concrete mixtures as two different components: the viscoelastic FAM and the elastic aggregate phase. He made the Superpave gyratory compacted FAM to represent the FAM phase placed in its corresponding asphalt concrete mixture. Then, he

tried to determine the mechanical properties of asphalt concrete mixture and its corresponding FAM phase. Dynamic modulus tests were then conducted on asphalt concrete samples to measure the dynamic modulus of mixtures, and torsional strain frequency sweep tests were performed on FAM samples to determine the dynamic modulus. It was found out that the results of FAM could reliably estimate the results of asphalt concrete mixture, and FAM could practically predict the behavior of the entire asphalt concrete mixture.

Im (2012) tried to understand the relation between mechanical characteristics (i.e., linear viscoelastic, nonlinear viscoelastic, and fracture properties) of asphaltic materials in mixture scale and component scale. To evaluate the mechanical characteristics of asphaltic materials in mixture scale, asphalt concrete samples were made, and FAM samples were fabricated to estimate the mechanical properties of asphaltic materials in component scale. Linear viscoelastic properties of asphalt concrete and its corresponding FAM phase were evaluated by performing dynamic modulus and frequency sweep tests on asphalt concrete and FAM samples, respectively. Additionally, viscoelastic properties of asphalt concrete mixtures and FAM were characterized by conducting creep-recovery tests at different stress levels. He reported that FAM results could reasonably estimate asphalt concrete mixture results; therefore, FAM could predict the mechanical characteristics of the entire asphalt concrete mixture.

Underwood and Kim (2013) performed an experimental study to determine the suitable composition of materials to use in multiscale modeling and experimentation. It was assumed that asphalt concrete is composed of a four-scale assemblage of components with different characteristic length scales; binder, mastic, FAM, and asphalt concrete. A series of direct microstructural experiments were performed. Figure 2-4 illustrates dynamic modulus versus frequency in four different length scales (i.e., binder, mastic, FAM, and asphalt concrete mixture).

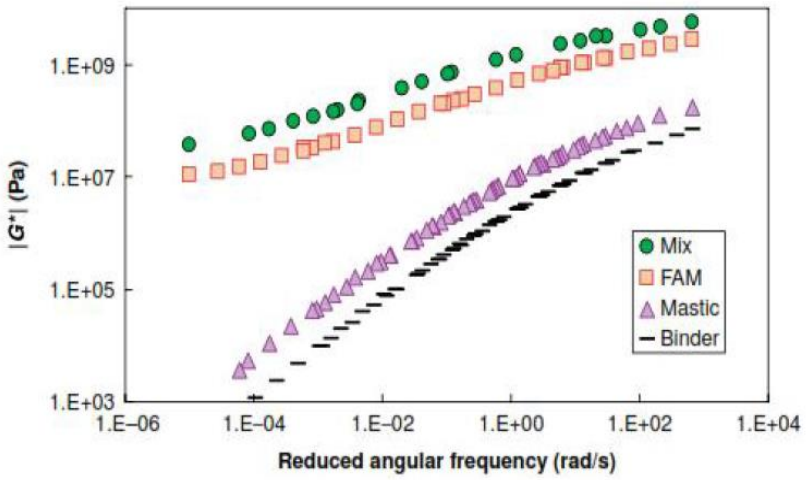

Figure 2-4. Asphalt concrete microstructure with two phases: coarse aggregates and fine aggregate matrix.

Im et al. (2015) found a linkage in the deformation characteristics between an asphalt concrete mixture and its corresponding FAM phase. A simple test procedure was designed and a simple

creep-recovery test was conducted at various stress levels on an asphalt concrete mixture and its corresponding FAM. The obtained test results of both mixtures (i.e., asphalt concrete mixture and FAM) were compared and analyzed using Schapery's single integral viscoelastic theory and Perzyna-type viscoplasticity with a generalized Drucker-Prager yield surface. They reported that there was a definite link between the asphalt concrete mixture and FAM in linear and nonlinear viscoelastic and viscoplastic deformation characteristics, and FAM could successfully predict the viscoelastic stiffness properties and viscoplastic hardening of asphalt concrete mixtures. Figure 2-5 depicts the linear viscoelastic creep compliance curves for the asphalt concrete mixture and its corresponding FAM phase before and after dimensionless process. The figure fully illustrates that results of the asphalt concrete mixture and FAM testing after the dimensionless process are approximately same.

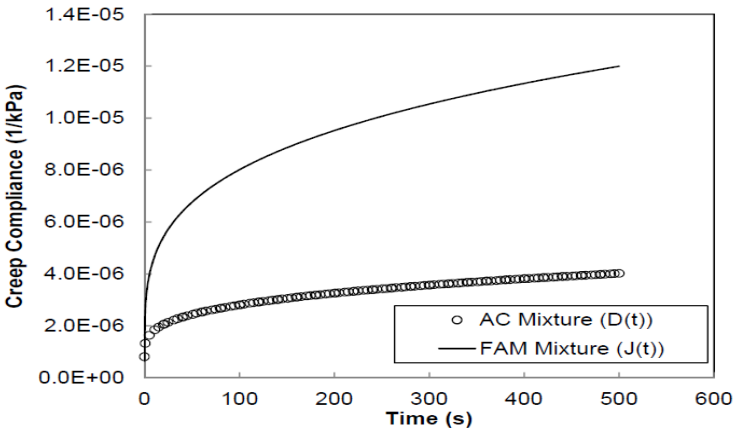

(a) before taking dimensionless process

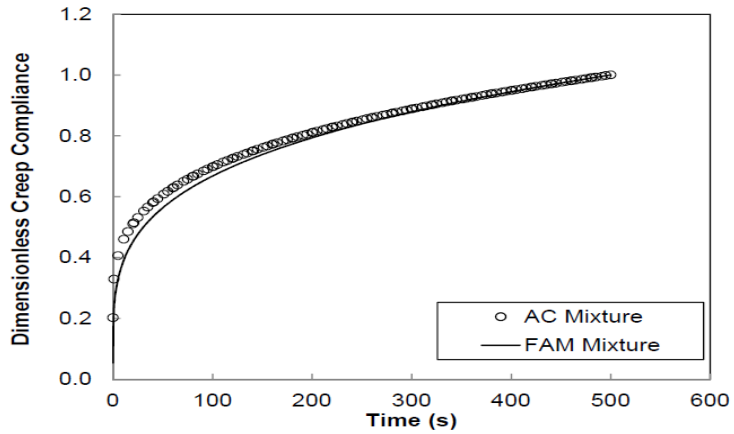

(b) after taking dimensionless process

Figure 2-5. Comparison of linear viscoelastic creep compliance curves (Im et al., 2015).

Chapter 3 Material Selection, Mixture Design, and Sample Fabrication

In this chapter, the materials used, mixture design, and the sample fabrication procedure are illustrated.

3.1 Materials

3.1.1 Rejuvenators and WMA Additive

Three different rejuvenators, obtained from petroleum, green, and agriculture technologies, and an amine-based WMA additive were employed in this study. The level of different rejuvenators added to the mixtures was based on manufacturers' recommendation. In Table 3-1, the specifications of the rejuvenators and WMA additive are listed.

Table 3-1. Rejuvenators and WMA Additive.

Additives	Type	ID	Description
Soybean Oil® (Archer Daniels Midland)	Agriculture Technology	R1	❖ dosage: 5% of virgin binder (or 1.6% of total binder) ❖ Added to virgin binder for HMA and WMA
Hydrolene® (HollyFrontier)	Petroleum Technology	R2	❖ dosage: 9% of RAP binder (or 6.2% of total binder) ❖ Added to virgin binder for HMA and WMA
Hydrogreen® (Meridian Chemicals)	Green Technology	R3	❖ dosage: 0.65% of RAP material (or 8.2% of total binder) ❖ Added to HMA batch
Evotherm® (Ingevity)	M1 Formulation	WMA	❖ dosage: 0.9% of virgin binder (or 0.29% of total binder) ❖ Added to virgin binder for WMA

3.1.2 Aggregates

Limestone, 2A gravel, and 3ACR crushed gravel (as the virgin aggregates) were mixed with a single source of RAP for the production of five mixtures. The nominal maximum aggregate size (NMAS) of the final aggregate blend was 12.5 mm. Table 3-2 summarizes the percentage of each aggregate source, its aggregate gradation, and the combined gradation.

Aggregates passing sieve No. 16 (1.18 mm) were selected for production of FAM, and they were also considered as the maximum aggregate size (MAS) in FAM. In this study, the FAM gradation was obtained from the original asphalt concrete mixture gradation by excluding aggregates larger than 1.18 mm (Table 3-3). It should be noted that only one source of virgin aggregate (3ACR

gravel) was used for the preparing the FAM because it was the dominant virgin aggregate in the asphalt concrete mixture. Also, 0.45-power gradation curves of the original asphalt concrete mixture and its FAM are presented in Figure 3-1.

Table 3-2. Mixture Information.

Material	% Agg.	Aggregate Gradation (% Passing on Each Sieve)								
		19mm	12.5mm	9.5mm	#4	#8	#16	#30	#50	#200
Limestone	11	100	50	45	43	30	20	2.7	2.5	2.1
3 ACR	17	100	100	100	98	80	39.5	24.2	14.6	5.9
2A	7	100	100	100	95	6.8	2.5	0	0	0
RAP	65	100	95.8	91.3	75	54.1	38.9	28.7	19.9	8.6
Combined		100	91.8	88.3	76.8	52.5	34.3	23.1	15.7	6.8

Table 3-3. Gradation Chart for FAM Mixture.

Material	% Agg.	Aggregate Gradation (% Passing on Each Sieve)			
		#16	#30	#50	#200
RAP	65	20	2.7	2.5	2.1
3 ACR	35	39.5	24.2	14.6	5.9
Combined		100	27.1	18.0	7.7

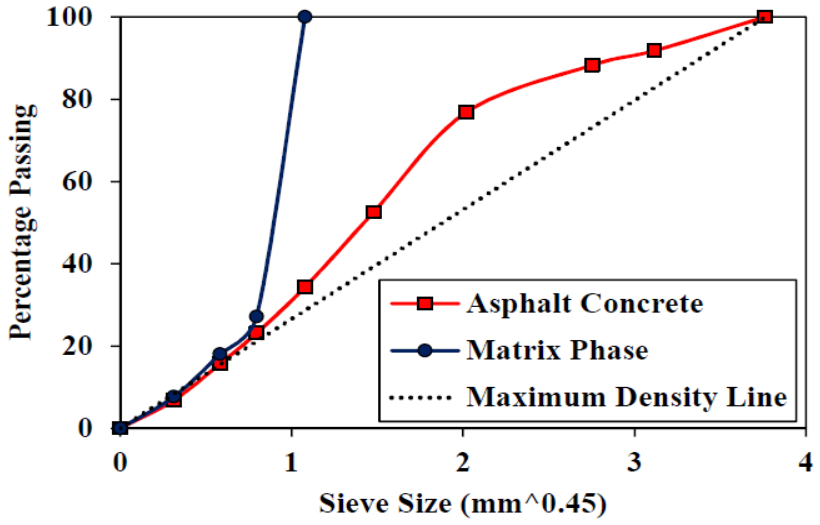

Figure 3-1. Virgin aggregate gradation curves: mixture and its fine aggregate matrix phase.

3.1.3 Binder

For the characterization of the old asphalt in the RAP, the old (aged) asphalt is separated from the RAP aggregates using a suitable solvent, and then it is retrieved from the solvent. In the extraction step, the RAP mixture (about 650 to 2,500 grams) was kept in contact with toluene (as the solvent), and this two-phase system was stirred for a sufficient time (see Figure 3-2). After the extraction step, the mixed sample (RAP mixture and toluene) was separated using a centrifuge. The centrifuge washing was repeated at least three times until the color of extracted material became the color of straw. To remove the fine particles from the extracted binder, micro-centrifugation was conducted as shown in Figure 3-3.

Figure 3-2. Extraction apparatus.

Figure 3-3. Micro-centrifugation of the solution after extraction.

In order to retrieve the asphalt binder from the solution, a rotary evaporator, equipped with distillation flask, was employed (Figure 3-4). At first the oil bath was heated up to 150 ± 5°C, and cooling water was circulated through the condenser. While the flask was above the oil bath, 200 to 300 mL of asphalt-toluene solution was drawn into the distillation flask by applying a vacuum of 72.0 ± 0.7 kPa. Then the flask was rotated at 40 rpm and lowered into the oil (approximately 40 mm into the oil bath). The vacuum was gradually decreased to 45.3 ± 0.7 kPa without allowing the solution to backflow into the condenser while applying vacuum. The 200 to 300 mL of asphalt-toluene solution was maintained in the flask until all the solution has entered the flask. The solution was gradually fed into the distillation flask. After distillation of the solvent, the vacuum was slowly increased to 6.7 ± 0.7 kPa. Carbon dioxide gas was then purged, and maximum vacuum was maintained for 45 ± 2 min. The flask was inverted and then placed into the oven at 165 ± 1°C to allow the asphalt binder to drain into a sample cup.

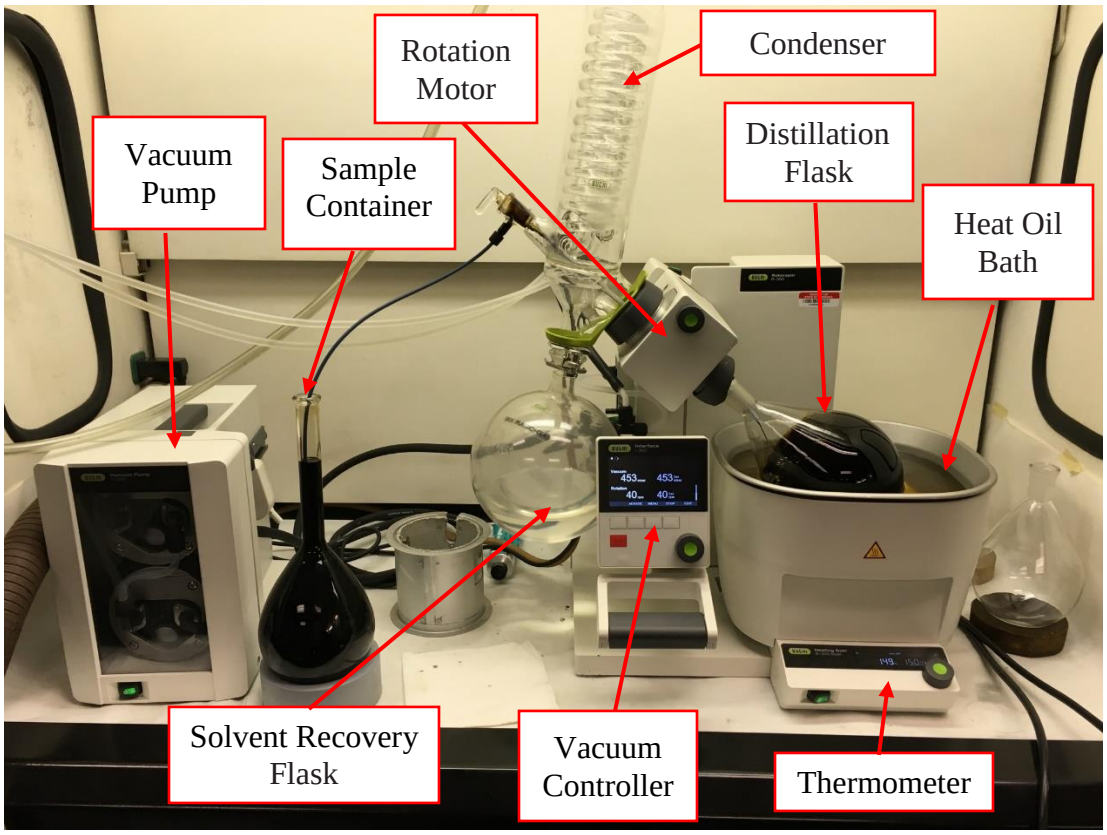

Figure 3-4. Rotary evaporator.

In addition to the recycle asphalt binder (RAB), a Superpave performance graded binder (PG 64-34) was used as a control binder (C). Asphalt mixtures with the RAB and C binder is hereafter designated as mixture CR. As mentioned in Section 3.1.1, three different rejuvenators, based on different production technologies (petroleum, green, and agriculture) and one amine-based WMA additive were also involved. Table 3-4 summarizes the information of seven binders and their corresponding seven asphalt mixtures.

Table 3-4. Binder Information Used in This Study.

Binder Description	Mixture ID
PG 64-34	C
VG 64-34 (35%) + RAB (65%)	CR
VG 64-34 (35%) + RAB (65%) + Rejuvenator No.1	CRR1
VG 64-34 (35%) + RAB (65%) + Rejuvenator No.2	CRR2
VG 64-34 (35%) + RAB (65%) + Rejuvenator No.3	CRR3
VG 64-34 (35%) + WMA Additive + RAB (65%) + Rejuvenator No.1	CWRR1
VG 64-34 (35%) + WMA Additive + RAB (65%) + Rejuvenator No.2	CWRR2

3.2 Mixture Design

3.2.1 Asphalt Concrete (AC)

Based on ignition test results, the percentage of remaining binder in the RAP material was 5.4%. With the combined aggregate blend, virgin binder, and RAP, a Superpave volumetric design of the mixture was conducted, which resulted in a binder content of 5.2% by weight of the total aggregate; this yields an air void content between 2.0 to 4.0% and a dust-binder ratio of 0.7 to 1.7%. In order to achieve the dust-binder ratio criterion, all virgin aggregates were washed by water before mixing, and then they were dried in the oven at 160 ± 3 ˚C for 24 hours. The mixing and compaction temperatures together with the heating and curing time are given in Table 3-5. Also, the mixture design for the seven mixtures is illustrated in Table 3-6.

Table 3-5. Mixing/Compaction Temperatures and Heating/Curing Time of HMA and WMA.

	Time in the oven (hours)		Oven temperature (˚C)	
	HMA	WMA	HMA	WMA
Virgin Aggregate	2	2	160±3	138±3
Virgin Binder	2	2	160±3	138±3
RAP	2	2	160±3	138±3
Curing	2	2	138±3	127±3
Compaction	-	-	138±3	127±3

Table 3-6. Mixture Design Results of Seven AC Mixtures.

Mixture Description	Mixture ID	G_{mm} (%)	G_{mb} (%)	VFA (%)	VMA (%)	Dust Content	Binder Content	D/B (%)	V_a (%)
virgin aggregates (35%) + RAP aggregates (65%) + virgin binder (PG 64-34)	C	2.449	2.402	77.4	12.7	6.7	5.10	1.32	2.9
virgin aggregates (35%) + RAP (65%) + virgin binder (PG 64-34)	CR	2.450	2.399	75.8	12.9	6.6	5.13	1.28	3.1
virgin aggregates (35%) + RAP (65%) + virgin binder (PG 64-34) + rejuvenator No.1	CRR1	2.445	2.409	79.4	12.5	6.8	5.09	1.33	2.6
virgin aggregates (35%) + RAP (65%) + virgin binder (PG 64-34) + rejuvenator No.2	CRR2	2.446	2.406	78.7	12.6	6.3	5.06	1.24	2.7
virgin aggregates (35%) + RAP (65%) + virgin binder (PG 64-34) + rejuvenator No.3	CRR3	2.454	2.406	77.1	12.5	6.4	5.11	1.25	2.9
virgin aggregates (35%) + RAP (65%) + virgin binder (PG 64-34) + rejuvenator No.1 + WMA	CWRR1	2.448	2.411	79.6	12.3	6.5	5.02	1.29	2.5
virgin aggregates (35%) + RAP (65%) + virgin binder (PG 64-34) + rejuvenator No.2 + WMA	CWRR2	2.445	2.412	80.7	12.3	6.1	4.96	1.23	2.4

3.2.2 Fine Aggregate Matrix (FAM)

The mixture design of FAM was conducted by using 65% RAP aggregate and 35% virgin aggregate based on Table 3-3. The process of the mixture design also included calculating the binder content, which was based on the RAP binder content.

The most challenging part of the FAM mixture design was to determine the proper amount of binder. To this end, a rational assumption was made: the ratio of RAP aggregate to virgin aggregate is equal to the weight ratio of RAP binder to virgin binder, as illustrated in Eq. 3.1:

$$W_{vb} = (P_{va} / P_{ra)} * W_{rb} \quad \text{Eq. 3.1}$$

where W_{vb} = weight of virgin binder,
W_{rb} = weight of RAP binder,
P_{va} = percentage of virgin aggregate, and
P_{ra} = percentage of RAP aggregate.

As mentioned earlier, 65% RAP aggregate and 35% virgin aggregate were used to make the FAM specimens. The percentage of old binder in the RAP mixture passing sieve No.16 was measured as 9.34% by weight of RAP through an ignition oven test. Based on these test results, weight of virgin binder could easily be calculated. For example, if the mixture contains 260 grams RAP aggregate (65%) and 140 grams virgin aggregate (35%), the weight of virgin binder would be 14.42 grams since RAP contains 9.34% old binder. This results in the weight of RAP being 286.79 grams and the weight of old binder being 26.79 grams in the mixture. Additionally, it should be noted that the percentage of virgin binder was also 9.34% by the weight of virgin aggregate passing sieve No. 16.

After determining the amount of virgin binder to be added in the FAM, the compaction density of FAM specimens should be determined. The compaction density of the FAM is defined as the ratio of mass of a FAM specimen to its volume as follows:

$$\rho_{FAM} = M_{FAM} / V_{FAM} \quad \text{Eq. 3.2}$$

where M_{FAM} = mass of FAM,
V_{FAM} = volume of FAM, and
ρ_{FAM} = density of FAM.

The bulk volume of each FAM specimen was calculated as 5.654 cm^3. Also, the compaction density of the FAM specimen was determined as 2.122 gr/cm^3 based on the volumetric design of the FAM phase of the AC mixture. By knowing the compaction density and the volume of each FAM specimen, the weight of each specimen was easily obtained using Eq. 3.2.

3.3 Specimen Fabrication

3.3.1 AC Specimens

3.3.1.1 Dynamic modulus and dynamic creep specimens

As illustrated in Figure 3-5, for the dynamic modulus and dynamic creep tests, a Superpave gyratory compactor was employed for the fabrication of the cylindrical samples with a diameter of 150 mm and a height of 170 mm. The compacted samples were then cored and sawed to produce testing specimens (diameter of 100 mm and a height of 150 mm) targeting an air void percentage of 4% ± 0.5%. In order to measure the axial displacement of the specimen during the tests, epoxy glue was used to fix mounting studs on the surface of the specimen so that the three linear variable differential transformers (LVDTs) could be attached to the surface of the specimen at 120^{o} radial intervals with a 70 or 100mm gauge length. Next, the specimen was mounted in the testing station for testing.

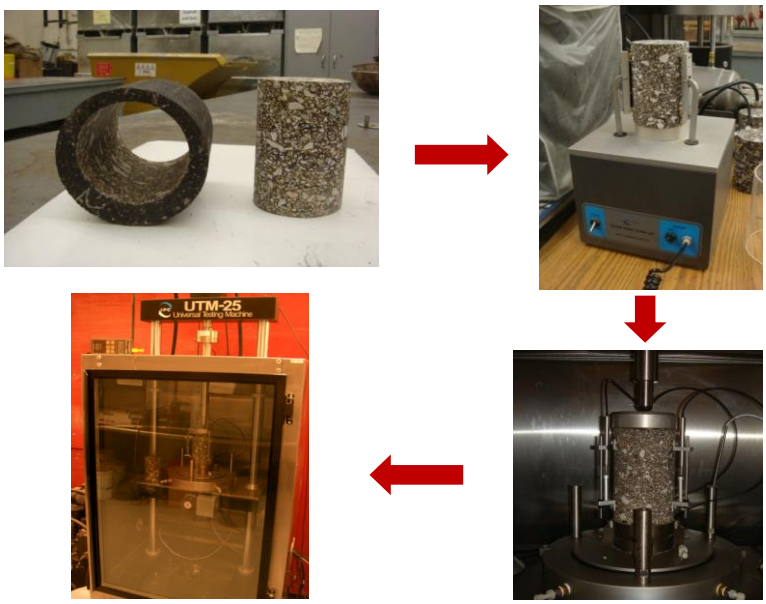

Figure 3-5. Specimen fabrication for dynamic modulus and dynamic creep tests of AC.

3.3.1.2 Semi-circular bend fracture test specimens

Figure 3-6 shows the specimen production procedure and the SCB fracture test configuration. The Superpave gyratory compactor was used to produce tall compacted samples, at 150 mm in diameter and 170 mm in height. Three slices (each with a diameter of 150 mm and a height of 50 mm) were obtained by cutting the top and bottom parts of the sample. Finally, the slice was cut into two identical halves, and a vertical notch (15 mm long and 2.5 mm wide) was prepared by the use of a saw machine.

(a) **(b)** **(c)** **(d)**

Figure 3-6. SCB specimen fabrication process: (a) compacting, (b) slicing, (c) notching, and (d) fracture testing configuration.

3.3.2 FAM Specimens

First, the virgin aggregates, RAP, and the binder were preheated at a pre-determined mixing temperature for 75 minutes and thoroughly mixed with each other. The mixing temperature was determined at 160˚C for all four mixtures (CR, CRR1, CRR2, and CRR3). The mixing process was conducted manually, since the amount of materials were small (approximately 500 grams). Second, the required amount of mixture to make each FAM specimen was heated up at a predetermined compaction temperature for 30 minutes. The compaction temperature was set at 138 ˚C. In the next step, the loose FAM mixture was evenly distributed in a specially designed and fabricated mold and compacted manually. Next, the mold was put in a freezer at a temperature of -18 ˚C for 10 minutes to cool it down in order to facilitate specimen removal from the mold without undue distortion of specimens. Then, the specimen was removed from the mold and placed at a room temperature of 25 ˚C for 24 hours. Finally, epoxy glue was used to secure holders to the specimen to make specimens ready for testing. After gluing, the specimen was placed at the room temperature of 25 ˚C for 5 hours. These specimen fabrication steps are summarized in Table 3-7.

Table 3-7. Procedure to Fabricate FAM Specimen.

Steps	Temperature (˚C)	Time
Pre-heating	160 and 138	75 min
Mixing		
Heating	138 and 127	30 min
Compacting		
Cooling	-18	10 min
Equilibration	Room temperature	24 hours
Gluing		
Equilibration	Room temperature	5 hours

FAM specimens were compacted in a cylindrical shape as shown in Figure 3-7. The cylindrical sample geometrics were implemented in this study for easy data analysis and to prevent complex stress distributions. The specification of each FAM specimen is presented in Table 3-8. 12 grams of loose FAM mixture material was calculated to obtain compaction density to make each compacted specimen 50 mm long with a 12-mm diameter.

Figure 3-7. FAM specimens: 12 grams (mass), 50 mm long, and 12 mm in diameter.

Table 3-8. FAM specimen Specifications.

Height	50 mm
Diameter	12 mm
Weight	12 gr
Percentage of binder	9.34%
Weight of RAP aggregate	7.07 gr
Weight of RAP binder	0.73 gr
Weight of virgin aggregate	3.81 gr
Weight of virgin binder	0.39 gr
Specific density	2.122 gr/cm^3

For torsional testing, two fixtures were secured to both ends of each FAM specimen using epoxy glue. Gluing was done carefully to avoid any undesirable stress concentrations at both ends. Moreover, during the gluing process, it was considered that fixtures should be in line. To this end, a small tool was designed and fabricated to make sure the two fixtures lined up Figure 3-8 and Figure 3-9 illustrate the FAM specimens with fixtures glued and the tool to line up the fixtures.

Figure 3-8. Fine aggregate matrix specimens with holders.

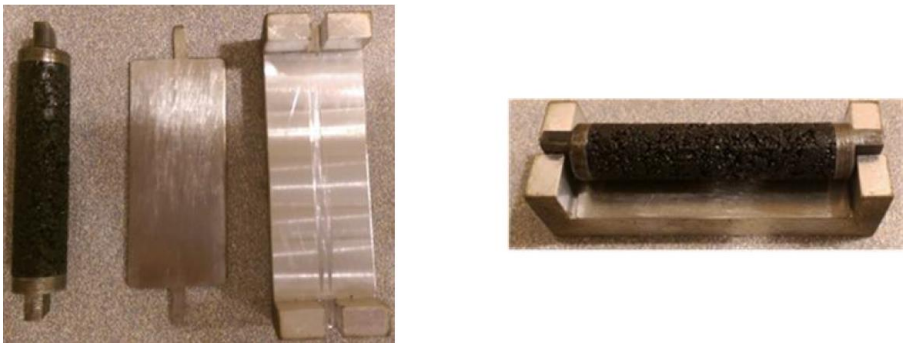

Figure 3-9. The tool to make holders line up.

Chapter 4 Laboratory Tests and Data Analysis

This chapter describes laboratory tests conducted for this study and test results. Various laboratory tests, including dynamic modulus, dynamic creep, SCB fracture test on AC, three types of strain-controlled torsional oscillatory shear tests (i.e., strain sweep, frequency sweep, and time sweep), and static creep-recovery tests on FAM were performed to compare the performance behavior of different asphalt mixtures. In the case of asphalt binders, four tests were performed using the dynamic shear rheometer (DSR), atomic force microscopy (AFM), Fourier transform infrared (FTIR) spectroscopy, and the saturates-aromatics-resins-asphaltenes (SARA) analysis. The last section of this chapter explores a linkage between the AC mixtures and their corresponding FAM mixtures.

4.1 Asphalt Concrete (AC) Tests and Results

4.1.1 Dynamic Modulus Test

The dynamic modulus test was conducted to characterize the linear viscoelastic material properties of the asphalt mixtures. The test was conducted using a universal testing machine (UTM 25 kN). The test procedure followed the standard, AASHTO TP79 (AASHTO, 2008; AASHTO, 2011). Three temperatures of 4, 20, and 40 °C and six or seven loading frequencies of 25, 10, 5, 1, 0.5, 0.1, and 0.01 Hz (40 °C only) were used, and the frequency-temperature superposition concept was applied to obtain the linear viscoelastic master curves at a target reference temperature of 20 °C. Two replicates were tested, and average values of dynamic modulus at each different testing temperature over the range of loading frequencies were obtained. As presented in Figure 4-1, adding rejuvenators to the CR mixture makes the mixture softer. Furthermore, among different rejuvenators investigated in this study, the petroleum-tech rejuvenator has a significant effect on CR mixture softening. The control mixture (C), where aged materials were not involved, was more ductile than all others over the entire span of loading frequencies. The effect of WMA additive (Evotherm in this study) was similar for the two different mixtures: CWRR1 (with the agriculture-tech rejuvenator) and CWRR2 (with the petroleum-tech rejuvenator).

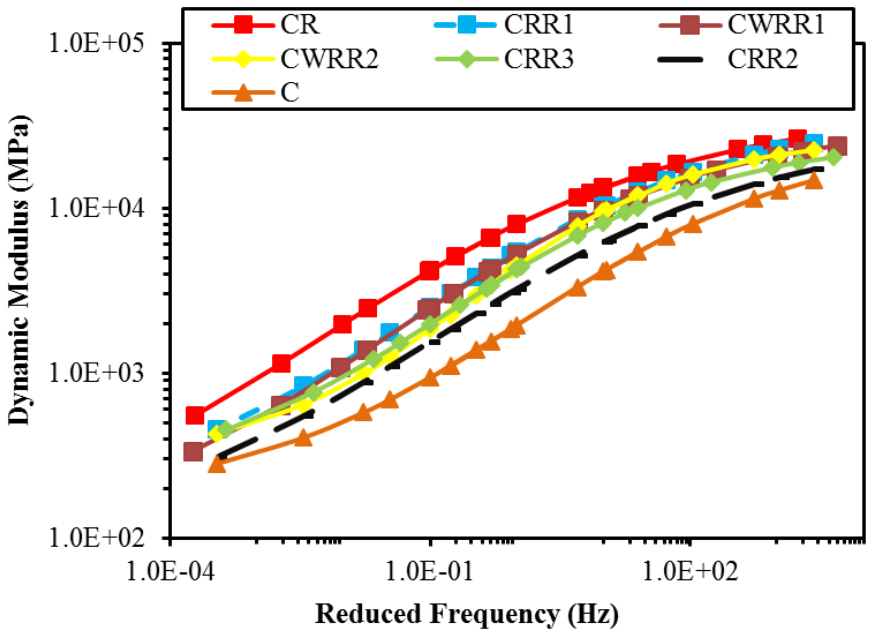

Figure 4-1. Dynamic modulus test results.

4.1.2 Dynamic Creep Test

In order to compare the permanent deformation behavior of AC mixtures, the dynamic creep test was conducted at 40 ˚C. The specimens employed for the dynamic modulus test were used according to AASHTO TP79 standard (AASHTO, 2011). The unconfined and repeated load test was performed under a deviator stress level of 138 kPa at 40 ˚C. The loading stress was applied in the form of a haversine curve with a loading time of 0.1 seconds in a rest period of 0.9 seconds in one cycle. Loading stress was repeatedly applied on the specimens until they exhibited a tertiary flow and reached 5% permanent strain level, or until the number of loading cycles reached 10,000. Two replicates for each mixture were tested (Figure 4-2). The accumulative permanent strain measured at 10,000 cycles of the CR mixture was approximately 80% lower than that of C mixture. The test results indicate that rejuvenators can lead to an increase in rutting potential since they usually make mixtures more compliant. More specifically, the agriculture-tech rejuvenator (R1) has the lowest effect compared to others (R2 and R3). The petroleum-tech rejuvenator (R2) and green-tech rejuvenator (R3) have almost similar effects on the rutting potential of mixtures. As it can be seen in Figure 4-2, the addition of the petroleum-tech rejuvenator (R2) to the WMA mixture (CWRR2) decreases its rutting potential compared to its counterpart in hot mix asphalt (CRR2). It should be noted that the behavior of the WMA mixtures (CWWR1 and CWRR2) is almost similar in permanent deformation.

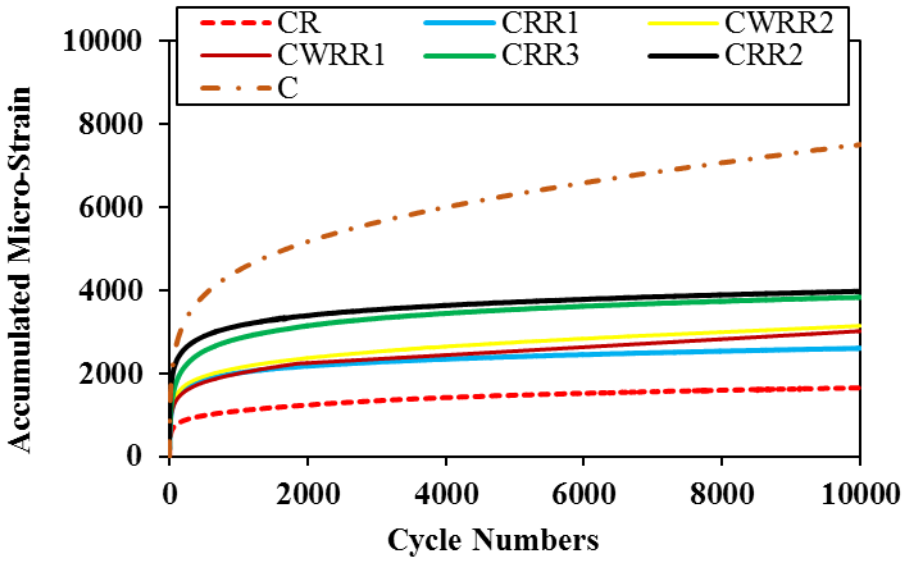

Figure 4-2. Dynamic creep test results.

4.1.3 SCB Fracture Test

Six SCB samples were prepared for each mixture. Three SCB samples were considered as the control sample without wet conditioning, and the other three samples were conditioned with water. Prior to testing, all six SCB samples were allowed to attain thermal equilibrium (targeting 25 ˚C) by putting them in the environmental chamber of the mechanical testing machine. Three samples were then saturated by water (70 – 80% saturation level). Then the wet samples (conditioned samples) were kept in the refrigerator at -18 °C for 16 hours. Following the freezing stage, the samples were submerged in water at 60 °C for 24 hours, and then in water at 25 °C for 2 hours. All dry (control) and wet (conditioned) samples were subjected to a simple three-point bending configuration with a monotonic displacement rate (5 mm/min) applied to the top center line of the SCB specimens at 25 °C. Figure 4-3 shows the results of SCB tests for seven mixtures.

The stiffness of asphalt mixtures is estimated from the upward slope (the slope up to peak) of the SCB load-displacement curve. However, there are different approaches for evaluating the fracture resistance of the mixtures from the SCB load-displacement curve. One of the conventional approaches is to estimate the fracture energy from the area under the load-displacement curve. The speed of crack growth/propagation rate by considering downward slope (the post-peak slope) is also a useful approach. This can also lead to the estimation of flexibility index (FI) to rank order cracking resistance of different AC mixtures as proposed by Al-Qadi et al. (2015):

$$FI = A \times \text{fracture energy} / \text{downward slope (m2)} \quad \text{Eq. 4.1}$$

where A is the calibration coefficient for unit conversions.

The values of fracture energy, FI, and the upward and downward slopes obtained from the SCB load-displacement curves are listed in Table 4-1. As can be seen, the peak and upward slope decrease by the addition of rejuvenators into the CR mixture indicating the softening effect of

rejuvenators on the high-RAP control mixture. This finding is in good agreement with several other studies (Al-Qadi et al., 2012; Im and Zhou, 2014).

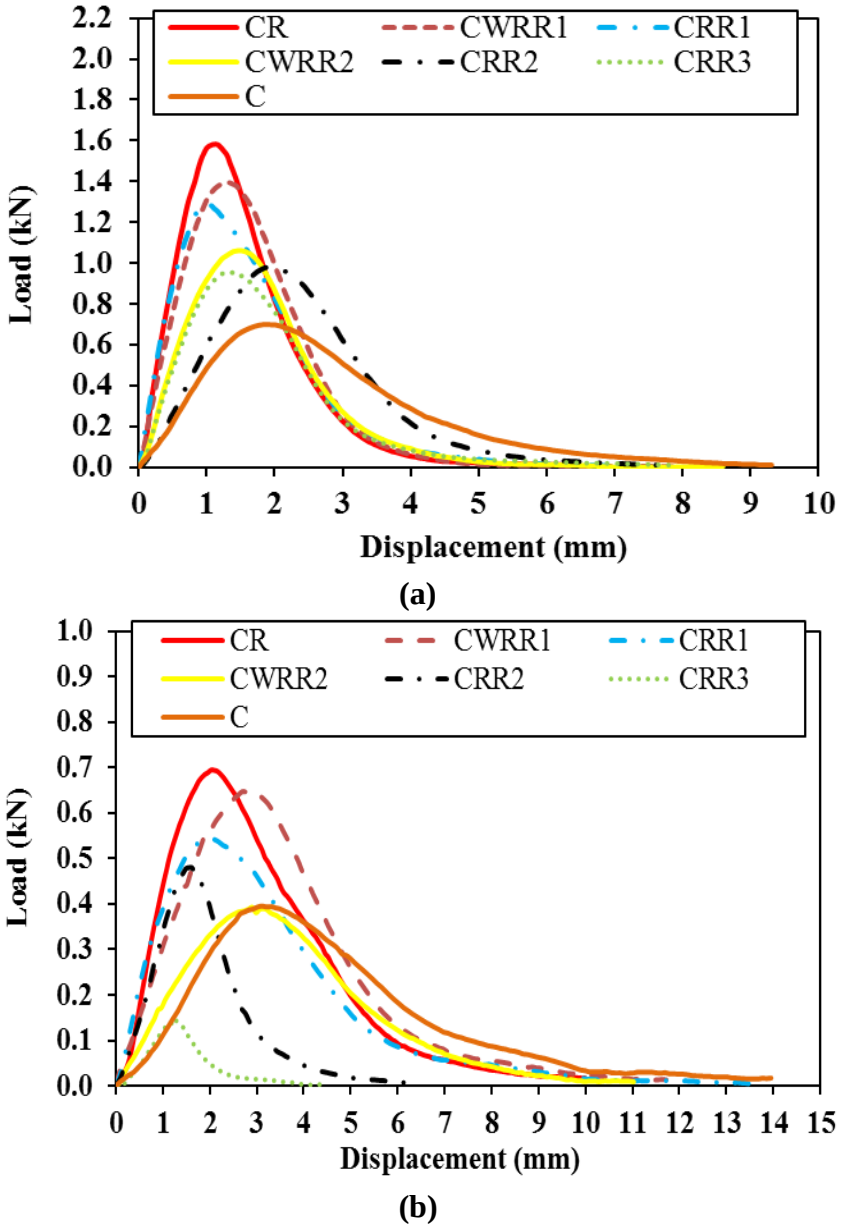

Figure 4-3. SCB curves for seven mixtures: (a) dry and, (b) wet condition.

It is noted that the evaluation of fracture behavior only based on the fracture energy can result in misleading information. For instance, the fracture energy of the CWRR2, CRR2, and CRR3 mixtures, as shown in Table 4-1 (dry condition), are very similar, but the FI indicates that the high-RAP mixture (i.e., CR) becomes somewhat more compliant with rejuvenators due to their softening effect. The increase of mixture ductility can improve cracking resistance of the CR mixture (Gibson et al., 2011; Im and Zhou, 2014; Zhou et al., 2014).

In the case of wet conditioned samples, the results of FI indicate that C and CR mixtures are less susceptible to moisture damage. Tran et al. (2012) also reported that the mixtures with a high content of RAP are less susceptible to stripping compared to the conventional asphalt mixtures, since the RAP aggregates have some pre-coating of asphalt, and this could prevent the penetration of moisture into the aggregates. As it can be seen in Table 4-1 (wet conditions), the addition of rejuvenators leads to a drop in FI values, which means the moisture resistance of rejuvenated mixtures has decreased. It should be noted that two samples modified by green tech and one sample modified by petroleum tech rejuvenator were failed during freezing-thawing cycle. Performance of agriculture-tech rejuvenator (R1) was better than other rejuvenators. Interestingly, the moisture resistance of WMA mixture with R1 decreased, while the petroleum-tech rejuvenator (R2) with the WMA additive showed increased moisture damage resistance.

Table 4-1. SCB Test Results.

Mixture ID	Upward Slope (m1)	Downward Slope (m2)	Fracture Energy (J/m^2)	Flexibility Index (FI)
Dry Condition				
C	0.425	-0.225	771	34.3
CR	1.472	-0.984	926	9.4
CRR1	1.276	-0.624	865	13.9
CRR2	0.593	-0.474	851	17.9
CRR3	0.735	-0.592	685	11.5
CWRR1	1.154	-0.850	950	11.2
CWRR2	0.767	-0.703	834	11.9
Wet Condition				
C	0.185	-0.093	654	70.3
CR	0.484	-0.158	903	57.0
CRR1	0.341	-0.165	712	43.1
CRR2	0.411	-0.338	453	13.4
CRR3	0.157	-0.148	193	12.9
CWRR1	0.310	-0.217	864	39.8
CWRR2	0.181	-0.120	568	47.4

4.2 FAM Tests and Results

A dynamic mechanical analyzer, AR2000ex rheometer, was used to perform tests on FAM mixtures. The machine had three main parts: a control computer, a testing station, and a system controller. The testing station is a main unit to conduct tests, and it has an environmental chamber to control testing temperature. The environmental chamber is connected to a nitrogen tank to control the temperature from -160 ˚C to 200 ˚C.

Three types of strain-controlled torsional oscillatory shear tests (i.e., strain sweep, frequency sweep, and time sweep) and a static creep-recovery test were performed on FAM specimens. First,

strain sweep tests were conducted to determine linear viscoelastic region in terms of the homogeneity concept. These tests also determined strain levels that produced maximum phase angles. Subsequently, frequency sweep tests were carried out to evaluate viscoelastic properties of each FAM mixture using strain levels within the linear viscoelastic region. Then, using strain levels larger than strains that satisfy linear viscoelasticity, time sweep tests were performed to evaluate fatigue resistance potential. Finally, static creep-recovery tests were conducted to determine the amounts of creep strain and irrecoverable strain of individual FAM mixtures at different stress levels. Table 4-2 and Table 4-3 present testing details.

Table 4-2. Strain-Controlled Torsional Oscillatory Shear Tests

Type of Test	Frequency (Hz)	Temperature (˚C)	Strain (%)	No. of Samples
Strain Sweep	0.1	40	0.0001 to 10	3
	10	25		3
	10	10		3
Frequency Sweep	0.1-10	10-20-30-40	0.001	3
Time Sweep	10	25	0.15, 0.30	3
			0.20, 0.35	3
			0.25, 0.40	3
Total Number of Samples				21

Table 4-3. Static Multiple Stress Creep-Recovery Test Procedure

Creep		Recovery		Temperature (˚C)	No. of Samples
Shear stress (Pa)	Time (sec)	Shear stress (Pa)	Time (sec)		
5	30	0	300	40	2
15	30	0	300	40	2
25	30	0	300	40	2
50	30	0	300	40	2
75	30	0	300	40	2

Each testing specimen was equilibrated for 30 minutes in the environmental chamber at the test temperature before doing the test to ensure that the inside temperature of the specimen in all areas was the same as the desired temperature to perform the test.

4.2.1 Torsional Shear Strain Sweep Test

Strain sweep tests were performed at different temperatures and frequencies, as presented in Table 4-4. Tests were started at 0.0001% strain and continued until specimen failure, and they were performed at three different frequency-temperature combinations; 0.1 Hz – 40 ˚C (compliant condition), 10 Hz – 10 ˚C (stiff condition), and 10 Hz – 25 ˚C (intermediate condition).

The first two frequency-temperature combinations were conducted to determine the linear viscoelastic region based on the homogeneity concept for the entire frequency and temperature domain that frequency sweep tests were performed. The Homogeneity concept clearly defined that the ratio of stress response to any applied strain was independent of strain magnitude. This concept could be considered for the strain sweep test by observing dynamic modulus as strain increases. Marasteanu and Anderson (2000) concluded that the linear viscoelastic region held until a 10% drop in the initial value of the dynamic modulus. The third frequency-temperature combination (i.e. 10 Hz – 25 ℃) was conducted specifically to carry out time sweep tests for determining strain levels that are considered large enough to cause nonlinear behavior (such as fatigue damage), because time sweep tests were conducted at 10 Hz and 25 ℃ to induce fatigue cracking.

The results of the strain sweep tests are illustrated in Figure 4-4. The results depict that the linear viscoelastic region held until around 0.01% strain, and the CR mixture had the stiffest behavior at all testing temperatures. Additionally, the petroleum-tech rejuvenated mixture showed the softest behavior between rejuvenated mixtures. Furthermore, linear viscoelastic dynamic shear moduli at three different test temperatures are presented in Table 4-4. It should be stated that strain sweep tests at a temperature of 10 ˚C were performed until approximately 0.03% strain, because at this temperature, specimens showed a very stiff behavior. The machine had reached the maximum torque capacity, and tests were ended at around 0.03% strain.

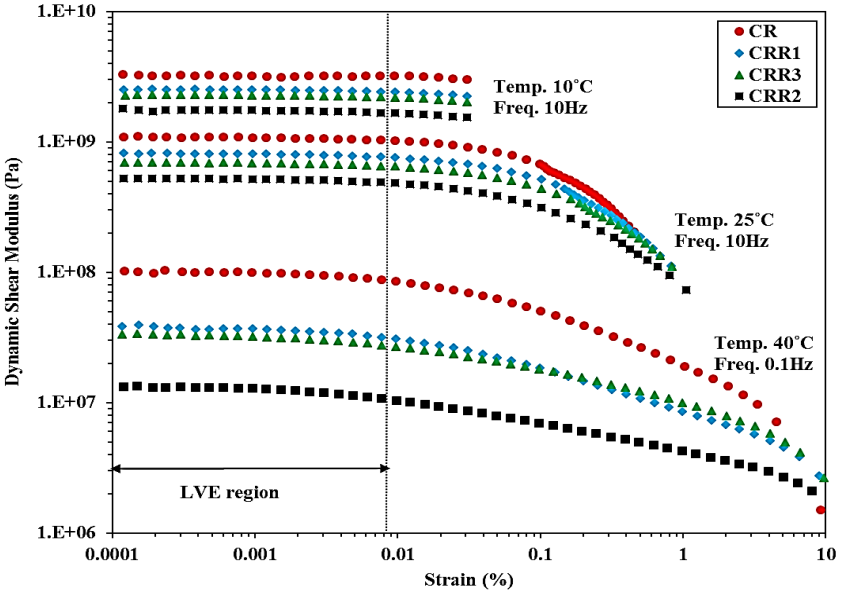

Figure 4-4. Torsional shear strain sweep test results at different frequency-temperature combinations.

Table 4-4. Linear Viscoelastic Dynamic Shear Modulus (Pa) at Three Test Temperatures

Mixture	Testing temperature (˚C)		
	10	25	40
CR	3.22E+09	1.19E+09	1.02E+08
CRR1	2.55E+09	8.66E+08	3.86E+07
CRR2	1.75E+09	5.27E+08	1.33E+07
CRR3	2.31E+09	8.24E+08	3.34E+07

4.2.2 Torsional Shear Frequency Sweep Test

Each frequency sweep test was performed by changing the loading frequency at a certain level of strain and temperature. In this study, frequency increased from 0.1 Hz to 10 Hz at each test to determine the effect of loading time on the stiffness of FAM, while the strain level was fixed at 0.001%. The strain level at 0.001% was low enough to prevent any nonlinear behavior with and without damage. Also, each specimen was tested at four different test temperatures (i.e., 10 ˚C, 20 ˚C, 30 ˚C, and 40 ˚C) to observe the effect of temperature on the stiffness of FAM mixtures.

Typical results of the frequency sweep test performed on mixture CRR3 are illustrated in Figure 4-5. The results showed that by increasing frequency, dynamic shear modulus increased, and by increasing temperature, dynamic shear modulus decreased. Also, Table 4-5 presents dynamic shear moduli for all four mixtures at 10 Hz and at the four different testing temperatures. The results indicated that the CR mixture had stiffer behavior than other mixtures, and the petroleum-tech rejuvenator had the softest behavior. Moreover, the petroleum-tech rejuvenated mixture (CRR2) showed softer behavior than agriculture-tech and green-tech rejuvenated mixtures, which showed similar behaviors.

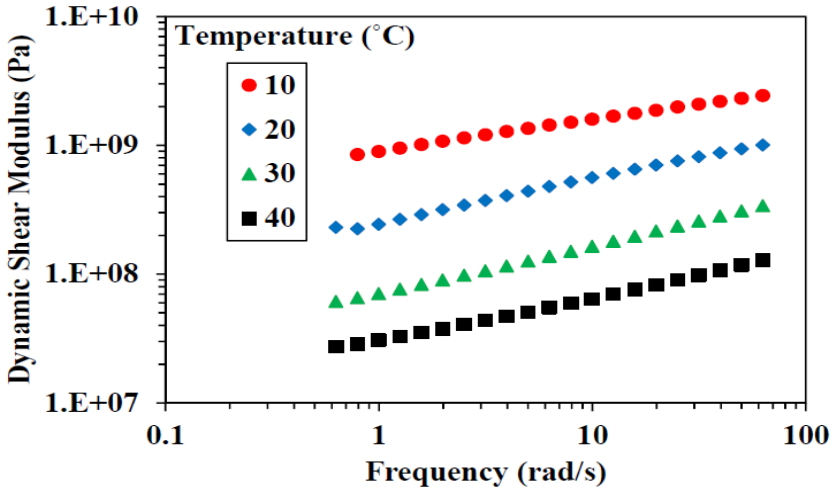

Figure 4-5. Results of the frequency sweep test at 0.001% strain on the mixture CRR3.

Table 4-5. Dynamic Shear Modulus at 10 Hz and Different Test Temperatures

Mixture	Dynamic shear modulus (Pa)			
	10 ˚C	20 ˚C	30 ˚C	40 ˚C
CR	3.10E+09	1.66E+09	8.26E+08	3.65E+08
CRR1	2.58E+09	1.25E+09	5.53E+08	2.13E+08
CRR2	1.77E+09	7.25E+08	2.77E+08	8.96E+07
CRR3	2.59E+09	1.12E+09	4.09E+08	1.60E+08

4.2.3 Torsional Shear Time Sweep Test

Time sweep tests were carried out to determine fatigue resistance of different mixtures. Tests were performed at 10 Hz and 25 ˚C with three different strain levels, and they were continued until the specimen failure and macro-cracks could be seen in the specimen by the end of the tests.

Since one of the main purposes of the time sweep tests was to create cracks in the specimens, strain levels were designated high enough to make cracks, and they were selected out of the linear viscoelastic region. Strain levels were selected based on two considerations: making fatigue cracks in the specimen at the end of the test, and finishing the test within a reasonable amount of testing time. Thus, three strain levels, 0.15%, 0.20%, and 0.25%, were selected for all four mixtures.

Typical results of time sweep tests performed on CRR3 mixture at a strain level of 0.25% are illustrated in Figure 4-6. As it can be distinctly seen in the figure and as mentioned by researchers (Branco, 2009; Kim et al., 2002; Kim et al., 2003; Kim and Little, 2005; Kim et al., 2003), there were three stiffness reduction steps in the time sweep test results: rapid reduction in early step, constant rate of reduction, and accelerated degradation step. Also, there were two inflection points: first inflection point (P_f) and second inflection point (P_s). These inflection points showed microcracking and macrocracking propagation in the specimen and changing material's behavior. P_f indicated microcracking development in the specimen with decreasing rate of stiffness, and P_s represented macrocracking propagation in the specimen. There was another point between the two inflection points, called transition point (P_t). P_t implied shifting from microcracking to macrocracking, and at this point the rate of stiffness reduction increased drastically.

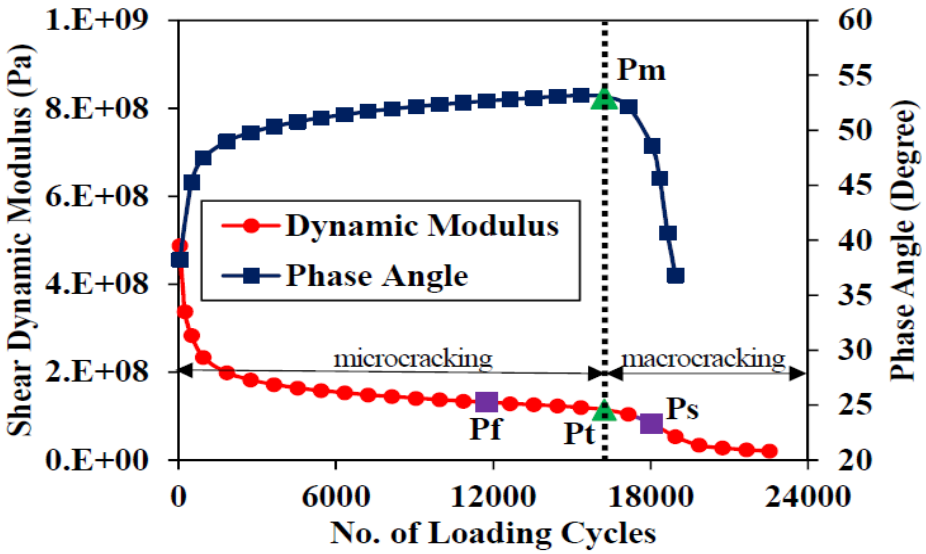

Figure 4-6. Dynamic shear modulus and phase angle vs. No. of loading cycles.

Regarding the time sweep test results, several studies (Kim and Little, 2005; Lee, 1996; Reese, 1997) investigated to identify a reasonable fatigue failure criterion. Lee (1996) indicated 50% loss in pseudo stiffness as the fatigue failure. Reese (1997) investigated fatigue failure based on changes in phase angle. Kim and Little (2005) performed time sweep tests on sand asphalt specimens containing different types of binders. They cross-plotted the number of loading cycles at the P_f, P_s, and P_t and the number of loading cycles at the maximum phase angle (P_m), and calculated the total deviation error. They considered the total deviation error as the total absolute deviation from the line of equality. They found out that the number of loading cycles at the transition point showed the minimum deviation error from the maximum phase angle, and the number of loading cycles at P_t could be considered as an acceptable fatigue failure. Therefore, it could be inferred that the number of loading cycles at the maximum phase angle was a fairly suitable fatigue failure criterion.

The phase angle of viscoelastic materials characterized the viscous nature of the materials, and the materials displayed more viscous behavior as the phase angle increased with more loading cycles because of microcrack generation. Consequently, the stiffness of the mixture decreased. When the phase angle reached its peak, microcracks coalesced into macrocracks, and it caused a substantial loss of structural integrity within the specimen. This transition resulted in a significant drop of phase angle as shown in Figure 4-7.

In this study, the number of loading cycles at maximum phase angle (or the number of loading cycles at the transition point) was considered as the fatigue life of the FAM mixture. Test results of the time sweep test were plotted on a log-log scale of the strain level versus the fatigue life for all four cases as shown in Figure 4-7. The results noticeably illustrated that rejuvenators increased the fatigue life of mixtures, and the petroleum-tech rejuvenated mixture showed greater fatigue resistance than the two other rejuvenated mixtures. Additionally, the mixture containing the petroleum-tech rejuvenator presented better fatigue resistance than the CR mixture.

Furthermore, the results distinctly displayed that the CR mixture had less fatigue resistance than the other mixtures, especially at lower strain levels, and green- and agriculture-tech rejuvenated mixtures showed shorter fatigue lives than the petroleum-tech rejuvenated mixture, especially at higher strain levels.

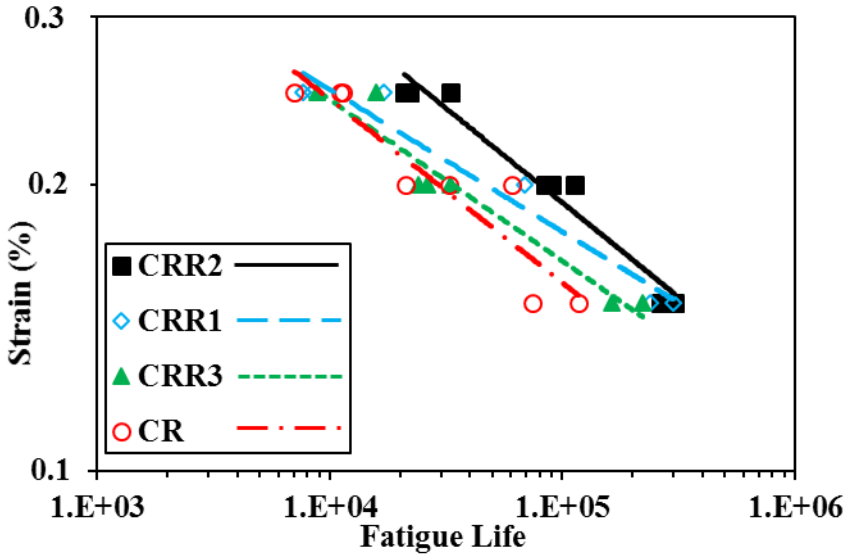

Figure 4-7. The strain level versus the fatigue life of each FAM mixture at 25 ˚C.

4.2.4 Static Multiple Stress Creep-Recovery Test

Static multiple stress creep-recovery tests were conducted to investigate stress-dependent permanent deformation characteristics of FAM mixtures. Thus, tests were performed at 40 ˚C. Creep loading time and recovery time were considered at 30 and 300 seconds, respectively. Tests were carried out in a wide range of creep stresses (i.e., 5, 15, 25, 50, and 75 kPa), and a static creep compliance, which was defined as the ratio of time-dependent strain to the applied static stress, was employed over the loading time to recognize the linear viscoelastic stress level in terms of homogeneity concept. Typical test results are presented in Figure 4-8 and Figure 4-9. Figure 4-8 illustrates that the linear viscoelastic region held until 15 kPa stress level, and after the linear viscoelastic stress level, creep compliance increased by increasing the applied stress level. Also, Figure 4-9 depicts that stress levels higher than the linear viscoelastic stress level caused larger creep strain and showed less recovery at the testing temperature. It should be noted that the linear viscoelastic region for all mixtures held until the 15 kPa stress level.

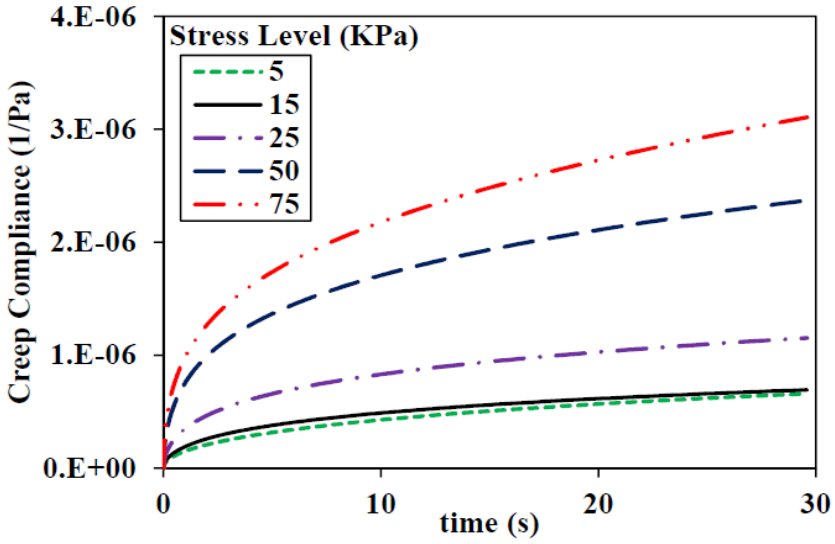

Figure 4-8. Creep test results to determine the linear viscoelastic stress level of the FAM mixture CRR3.

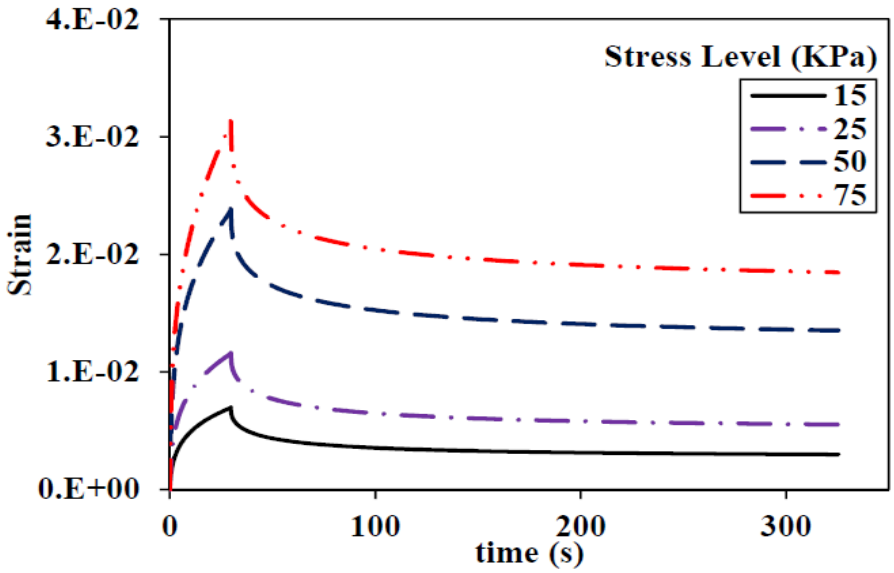

Figure 4-9. Creep-recovery test results of the FAM mixture CRR3.

The creep and creep-recovery test results of all four FAM mixtures at 25 kPa are compared in Figure 4-10 and Figure 4-11, respectively. The results indicated that the rejuvenated mixtures showed softer behavior than the CR mixture because they could develop more strain, and the petroleum-tech rejuvenator had more softening effect than the green-tech and agriculture-tech rejuvenators. Test results were in good agreements with other test results (i.e., strain sweep and frequency sweep tests) presented earlier.

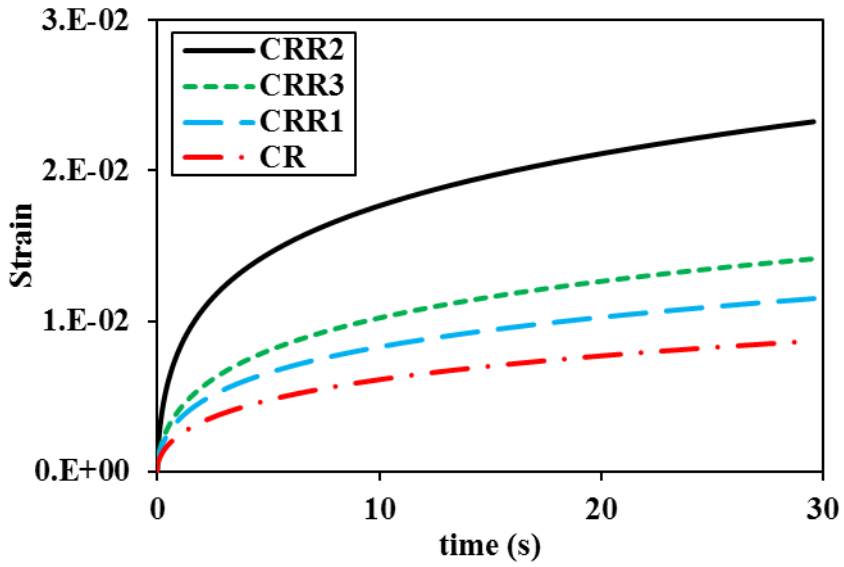

Figure 4-10. Creep test results of all mixtures at 25 kPa stress level.

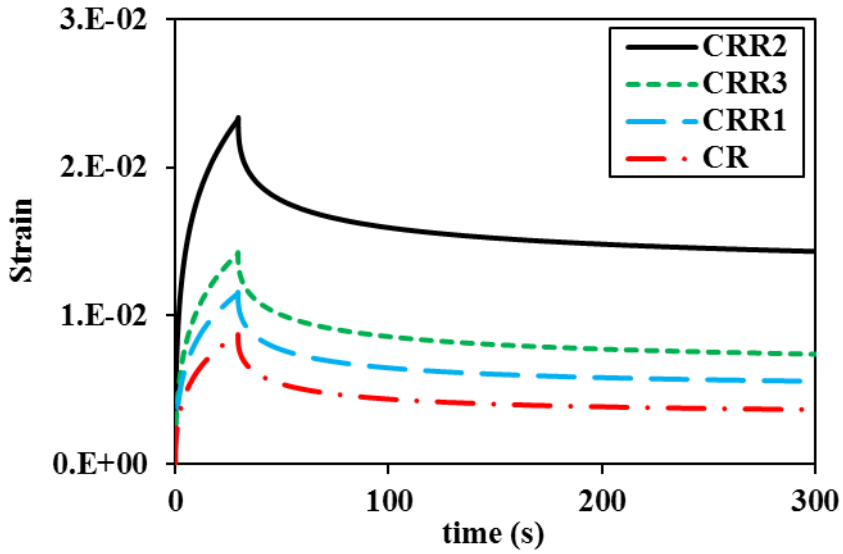

Figure 4-11. Creep-recovery test results of all mixtures at 25 kPa stress level.

4.3 Binder Tests and Results

For binder testing, a Superpave performance graded binder PG 64-34 as a control binder (C), an extracted binder from the RAP, three different rejuvenators based on different production technologies (i.e., petroleum, green, and agriculture), and one amine-based WMA additive (i.e., Evotherm) were chosen and used to compare the seven binder samples, as previously given in Table 3-4.

4.3.1 DSR Tests

Dynamic shear rheometer tests were performed on all the binder samples using the AR2000ex rheometer. Experimental investigations were carried out on the different binders to characterize the linear viscoelastic response. All the experiments conducted using the dynamic loading conditions were performed with the strain controlled mode using an 8-mm parallel plate geometry.

4.3.1.1 Strain sweep test

Strain sweep tests or linear amplitude sweep tests were performed to establish the linear viscoelastic regime whose results will subsequently be used in the frequency sweep tests. At first, strain sweep tests were conducted on each binder sample at 0 ºC and 45 ºC and at two different frequencies, 0.1 Hz and 10 Hz. At a given frequency and temperature, the strain was linearly increased from 0 to 10 %, and changes in dynamic shear modulus (|G*|) and phase angle (δ) values over increasing strains were recorded. If the sample were within the linear viscoelastic region, the modulus value |G*| and δ values would not change. Hence, the strain value at which changes in these values are considerable (such as more than 10%) would be regarded as the linear limit above which the samples would show nonlinear behavior (Kim et al., 2006). These test conditions were selected to ensure the samples were well within the linear viscoelastic region at the lowest and highest levels of testing temperatures (i.e., 0 ºC and 45 ºC) and loading frequencies (i.e., 0.1 Hz and 10 Hz) for the following frequency sweep tests. An example of the results from the test conducted at a temperature of 0 ºC and a frequency of 0.1 Hz is shown in Figure 4-12 (|G*|) and Figure 4-13 (δ). As expected, for a relatively stiff material, the modulus values are higher and the phase angle is lower. One can also infer that the CRR3 would be relatively more fluid-like material compared to others. The CR binder clearly shows the stiffest behavior. Based on these test results, a strain amplitude of 0.01% was selected for all subsequent frequency sweep tests.

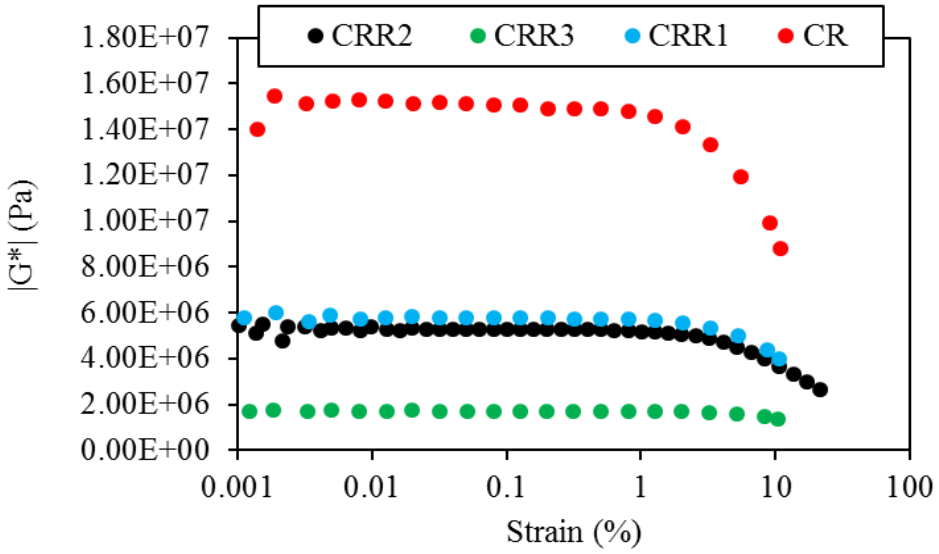

Figure 4-12. Values in a strain sweep test for different binders at 0 ºC and 0.1 Hz frequency.

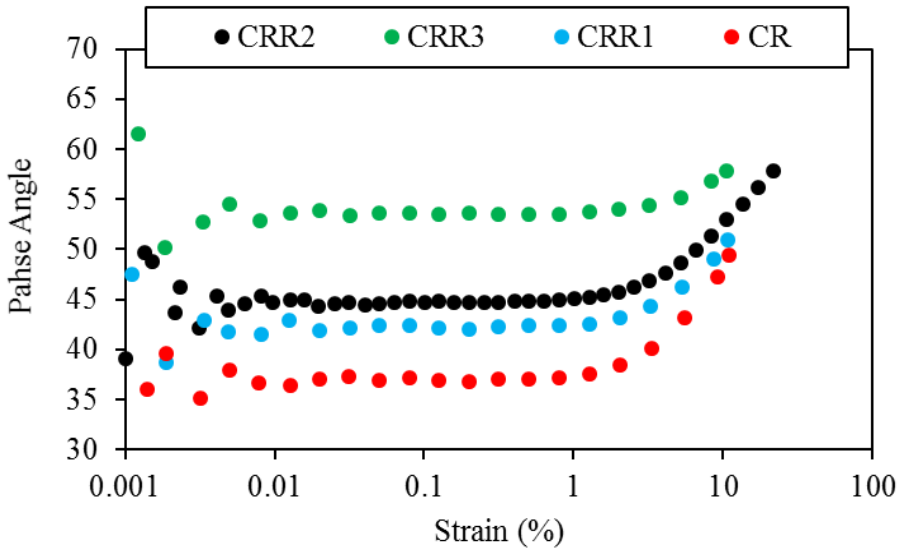

Figure 4-13. Phase angle (δ) values in a strain sweep test for different binders at 0 ºC and 0.1 Hz frequency.

4.3.1.2 Frequency sweep tests

Frequency sweep tests were conducted on each binder at four different temperatures (0 ºC, 10 ºC, 25 ºC, and 45 ºC), frequency ranging from 0.1 Hz to 10 Hz, and at a constant strain amplitude of 0.01%. Master curves were then obtained by shifting the curves at different temperatures to a reference temperature of 25 ºC (Ferry, 1980; Tschoegl, 2012). Figure 4-14 shows the plot of the master curves of all four binder samples. As shown, the mechanical behavior of the binders treated with the rejuvenator is quite different from binders without the rejuvenator. Adding the rejuvenator generally softened the aged binder, and the extent of influence is different owing to the nature of the rejuvenator. It can be seen that the impact of green-tech rejuvenator on softening of aged binder is more significant than the petroleum-tech and agriculture-tech rejuvenators.

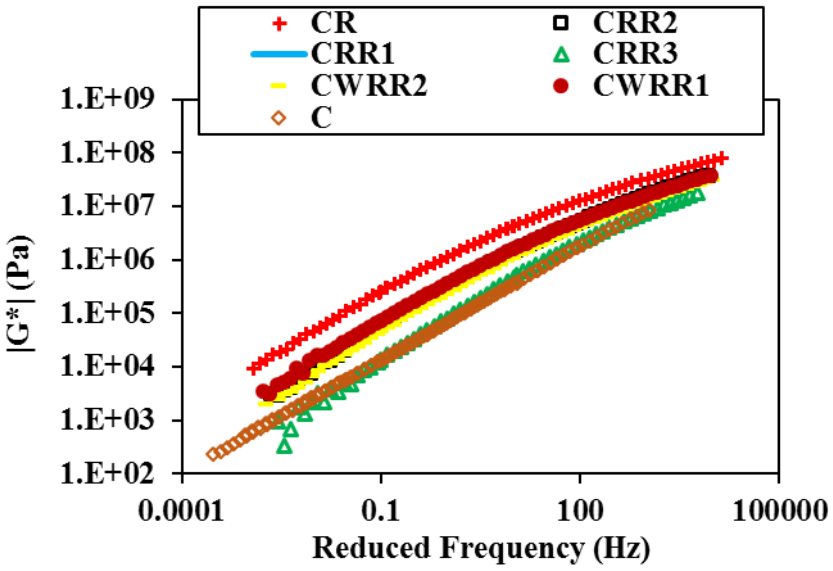

Figure 4-14. Master curve plot of all the binders at the reference temperature of 25 ºC.

4.3.2 AFM Tests

The Bruker Dimension Icon® Atomic Force Microscope was employed in this study (Figure 4-15). It is equipped with ScanAsyst® automatic image optimization mode based on PeakForce Tapping technology, which enables users to obtain consistent high-quality results easier and faster. The images obtained in the tapping mode were used to characterize the nano-/micro-structure of the asphalt binder after introducing the rejuvenators and WMA additives.

Figure 4-16 and Figure 4-17 illustrate the topographical and phase images of the binders. Asphalt binder is a mixture of hydrocarbons with a variety of functional groups, and it contains metals such as vanadium and nickel. The phase images reveal that the asphalt binder is a heterogeneous material. Also, there is a flat background in all images, and a second phase (dark color), which is not clearly distinguishable from the flat background, is dispersed through the matrix phase (Figure 4-16(a) and Figure 4-17(a)). Within the second phase (dark color), an elongated structure is observed, identified by a succession of pale and dark lines; this is a so-called "bee-shaped" structure. To have a better illustration of the shape of "bee-shaped" structure, a 2-D and 3-D topographical images of control binder (C) are shown in Figure 4-18.

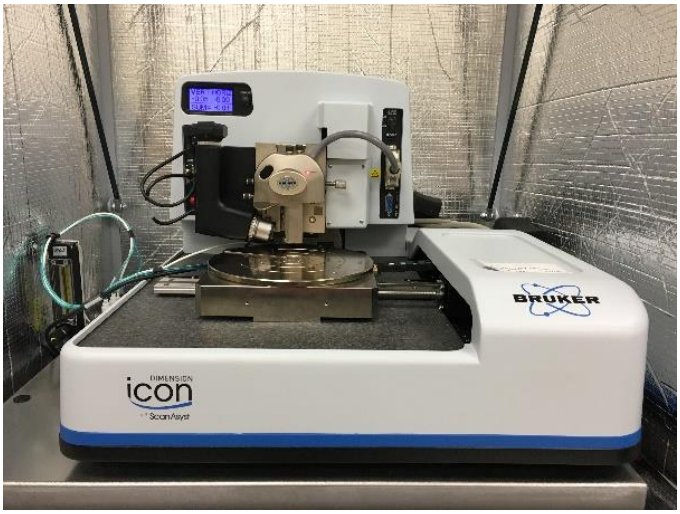

Figure 4-15. Bruker Dimension Icon® Atomic Force Microscope.

In previous other studies, the appearance of the "bee-shaped" structure has been attributed to the asphaltene content (Loeber et al., 1998; Zhang et al., 2011). However, Masson et al. (2006) reported that there is a high correlation between the area of the 'bee-like' structure and sum of the vanadium and nickel content in binder. To explore whether there is a correlation between the 'bee-like' structure and asphaltenes, control binder (C) was separated into two phases: asphaltenes and maltenes. Then the topographical image of control binder and maltenes phase was detected by AFM. The topographic image of control binder and maltenes phase (binder without asphaltenes) is shown in Figure 4-19. It is vividly observed that the 'bee-like' structure disappears in maltenes phase image. This observation implies that the appearance of 'bee-like' structure is related to the existence of asphaltenes in the binder. Asphaltene is a highly polar and heavy species of the asphalt binders; this species is soluble in aromatic solvents such as toluene and benzene but insoluble in aliphatic solvents (Petersen, 2000). The "bee-shaped" structure has also been considered as the microcrystalline waxy molecules present in asphaltenes, which crystallize during cooling to the testing temperature (Lu et al., 2005).

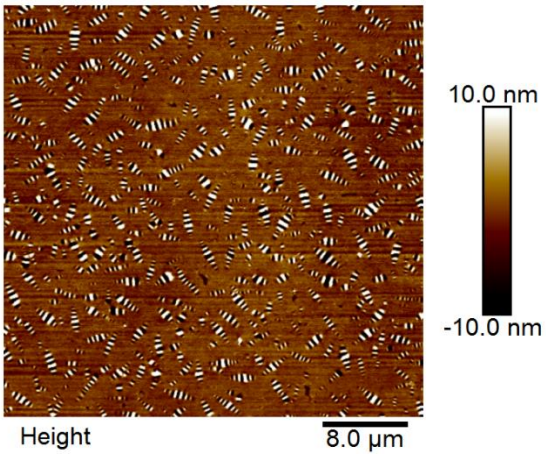

(a)

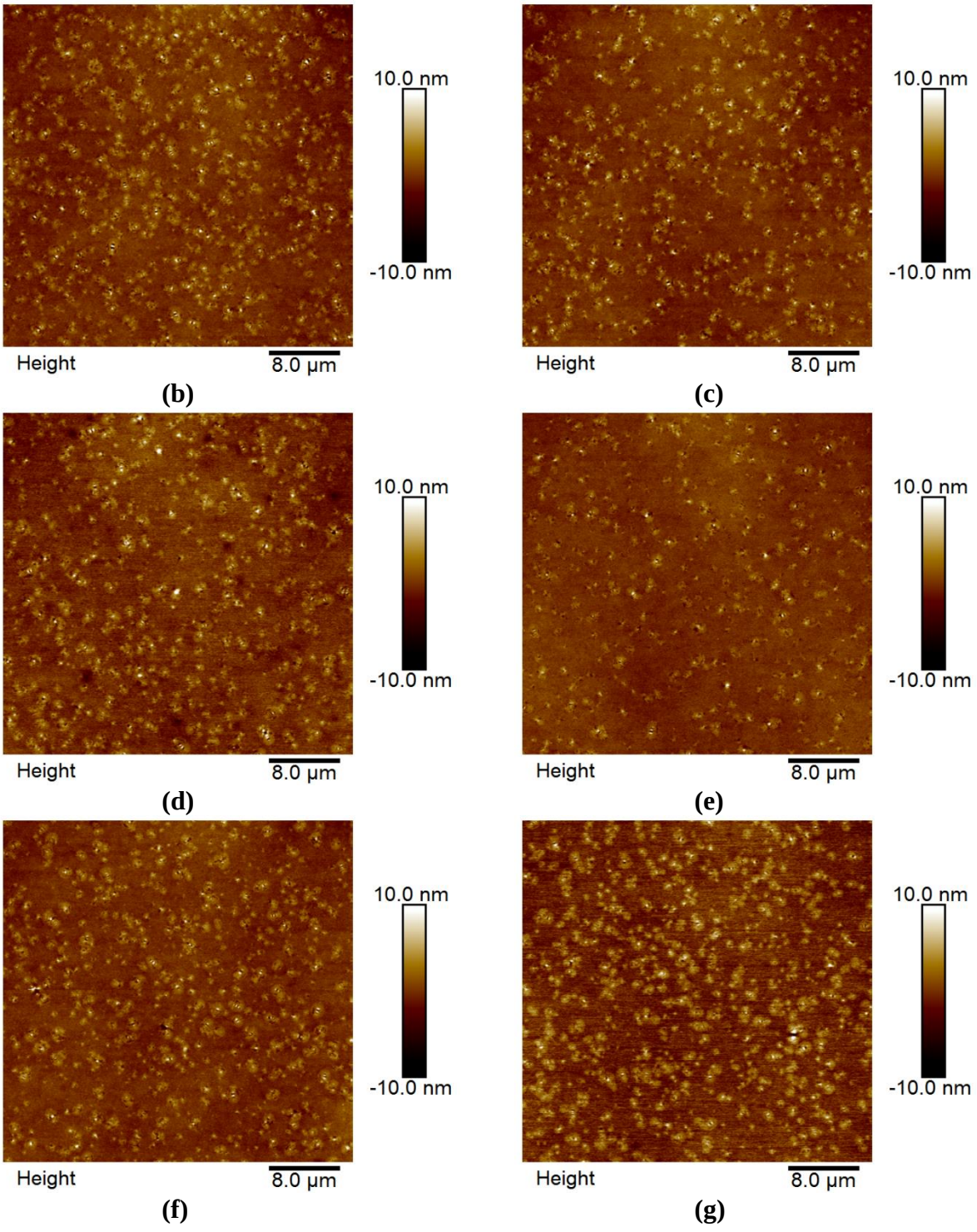

Figure 4-16. AFM topographical images of binders: (a) C, (b) CR, (c) CRR1, (d) CRR2, (e) CRR3, (f) CWRR1, and (g) CWRR2.

Figure 4-16(c) to (g) shows that by the addition of rejuvenators to the CR binder, the size and number of "bee-shaped" structure decrease, and they appear in small chains with much smaller width than those in the C and CR binders. However, the binders treated by WMA additive (CWRR1 and CWRR2) lead to an increase in the "bee-shaped" structure compared to their counterparts (CRR1 and CRR2). A comparison between the phase images of C asphalt binder (Figure 4-17(a)) and CR, shows that the color of flat matrix in C is lighter after adding RAB binder; this means that the CR binder is stiffer than C binder. Furthermore, the presence of rejuvenators in the CR asphalt binder (Figure 4-17(c) to (g)), results in a darker color of the flat matrix of rejuvenated binders compared to the CR; i.e. the flat matrix of rejuvenated binders is softer than CR.

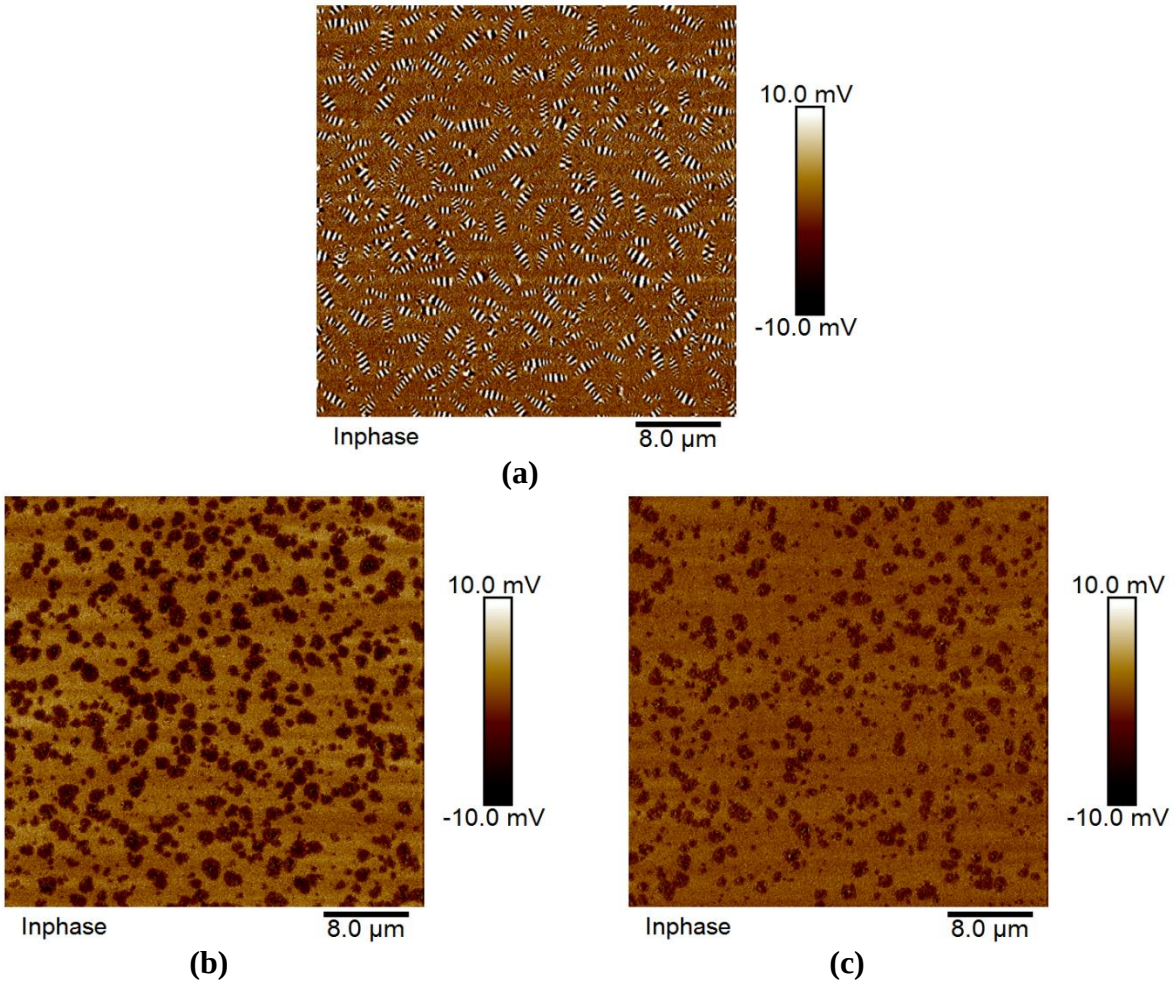

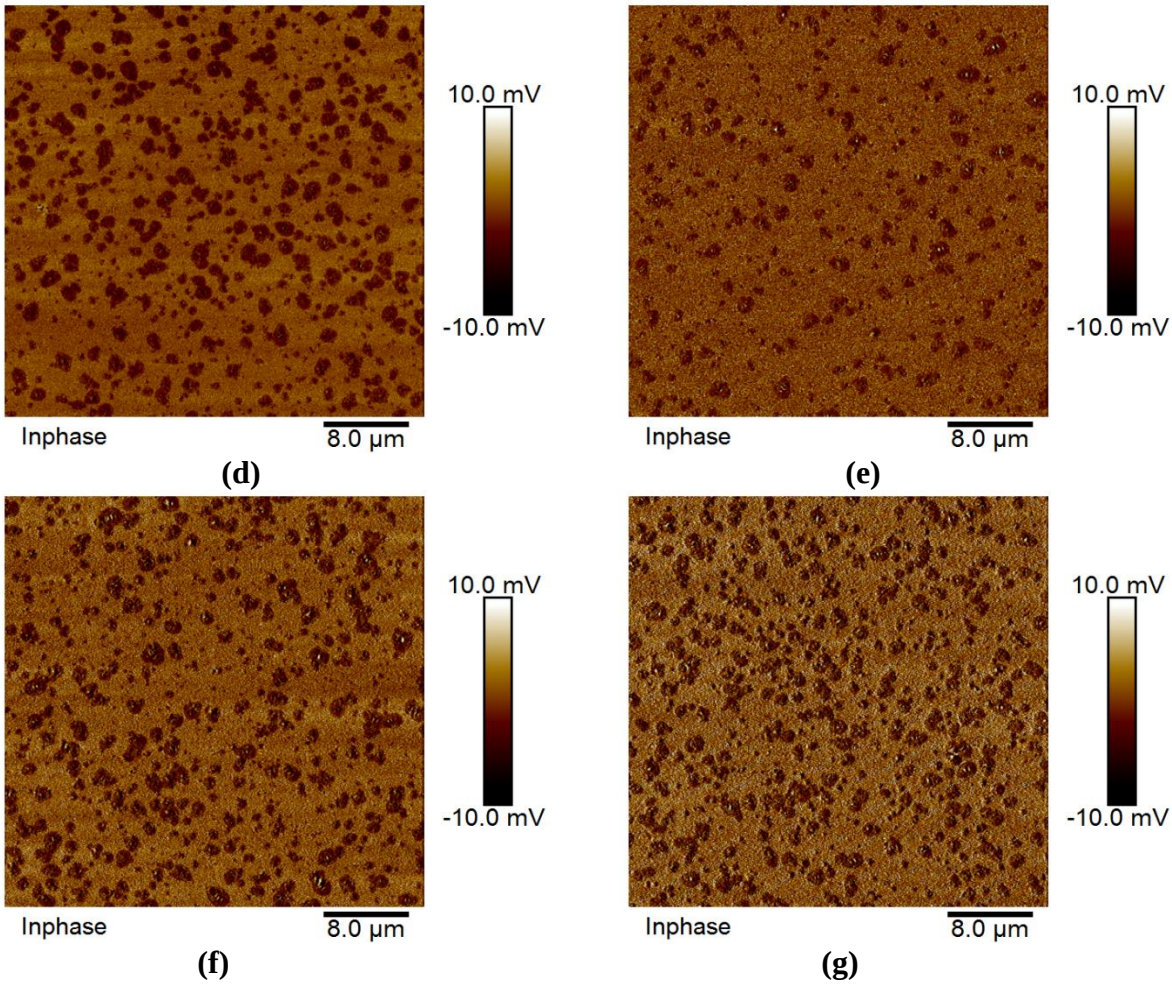

Figure 4-17. AFM Phase images of binders: (a) C, (b) CR, (c) CRR1, (d) CRR2, (e) CRR3, (f) CWRR1, and (g) CWRR2.

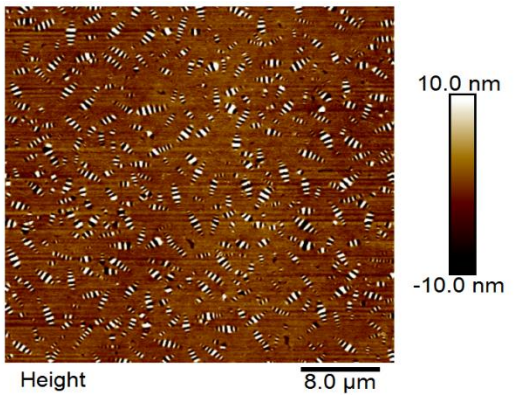

(a)

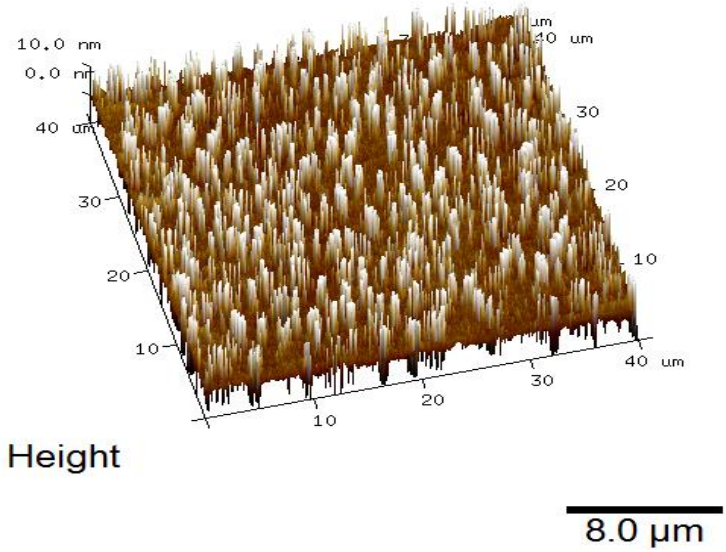

(b)

Figure 4-18. Topographical image of the control binder: (a) 2-D, (b) 3-D.

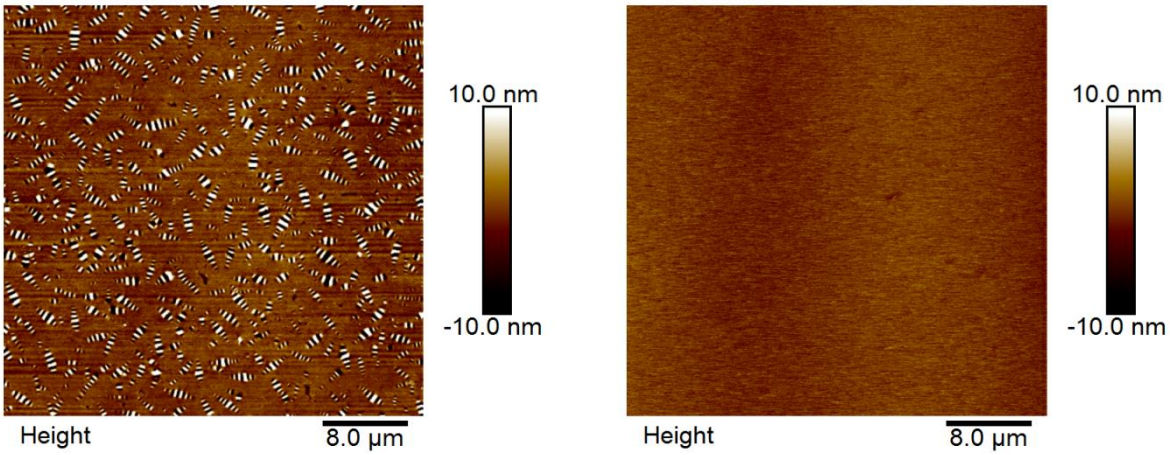

(a) **(b)**

Figure 4-19. Topographical image of the: (a) control binder, (b) control binder without asphaltenes.

4.3.3 FTIR Tests

Fourier transform infrared (FTIR) spectroscopy has been used to quantify the relative concentrations of characteristic functional groups present in bitumen that may be responsible for the aging process. By using FTIR, a better understanding of the interaction between the rejuvenator and binder can be established. The increase in absorbance, and thus relative concentrations, of two functional groups (carbonyl groups and sulfoxide groups) have been widely used as oxidation indicators (Lamontagne et al., 2001; Mouillet et al., 2008). The formation of these polar functional groups resulted in an increase of intermolecular forces between the fractions, thus increasing viscosity (Claine Petersen, 1998; Petersen and Glaser, 2011) and also increasing the level of large and heavy molecules due to molecular association (2002).

FTIR spectroscopy of the binders and rejuvenators were conducted with a Thermo Nicolet Avatar 380 FTIR spectrometer. The FTIR was in the attenuated total reflection (ATR) mode using a Smart Performer ATR accessory with a diamond crystal, allowing for facile IR acquisition of liquids and solids. Each spectrum was taken from a range of wavenumbers from 400 to 4,000 cm^{-1} with a resolution of 4 cm^{-1}. For the estimation of the areas under the peaks, the OMNIC 8.1 software was used. The background spectrum was subtracted from each sample spectrum. The diamond crystal was cleaned with ethanol after each sample analysis. The FTIR spectra of all seven binders are shown in Figure 4-20.

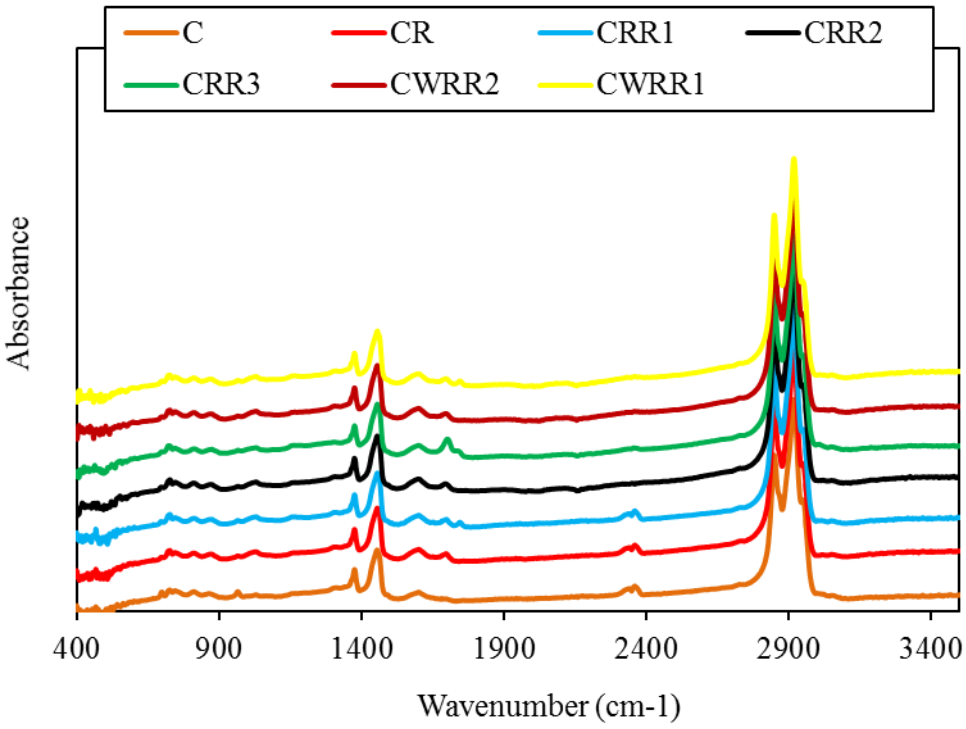

Figure 4-20. FTIR spectra of all seven binders.

The area under each characteristic wave number (corresponding to functional groups) was estimated for the determination of structural indices, ratios of the area under a specific band to the overall area. These structural indices can be logically employed for comparative purposes. The

calculation of structural indices adapted from Lamontagne et al. (2001) and Feng et al. (2016) can be described as follows:

Carbonyl Index ($I_{C=O}$): A_{1700} / ΣA
Sulfoxide Index ($I_{S=O}$): A_{1032} / ΣA
Aliphatic Index (I_{Al}): (A_{1460} + A_{1377}) / ΣA
Aromatic Index (I_{Ar}): (A_{1600}) / ΣA
Aromatic to Aliphatic Ratio = A_{1600} / (A_{1460}+ A_{1377})

where $\Sigma A = A_{1700} + A_{1600} + A_{1460} + A_{1377} + A_{1032} + A_{956} + A_{866} + A_{814} + A_{723}$

Each structural index calculated from the FTIR test results are shown in Figure 4-21. Two important functional groups, carbonyl (C=O) and sulfoxide (S=O), are the criteria for relative oxidation during the aging process. The strong intermolecular forces between these polar functional groups results in an increase in the viscosity (Claine Petersen, 1998; Petersen and Glaser, 2011). As can be seen in Figure 4-21 (a), (b), (c), and (d), after blending the RAP-extracted binder (i.e., RAB) with the control binder (C), namely CR, the two oxidation indices (carbonyl and sulfoxide) and aromatic index increased, whereas aliphatic index decreased. Interestingly, introducing the agriculture-tech and petroleum-tech rejuvenators (i.e., R1 and R2) to the binder CR resulted in a decrease in the carbonyl, sulfoxide and aromatic indices and an increase in aliphatic index. This indicates that the rejuvenators can restore the chemical compositions of the CR binder. The impact of the green-tech rejuvenator (R3) was quite different from the other two rejuvenators. As can be seen in the figure, the carbonyl index of CRR3 was greater than that of CR, which was opposite from the binders mixed with the other two rejuvenators. The aliphatic index of the CRR3 decreased from the value of the CR; however, the two other rejuvenators increased the aliphatic index of the CR.

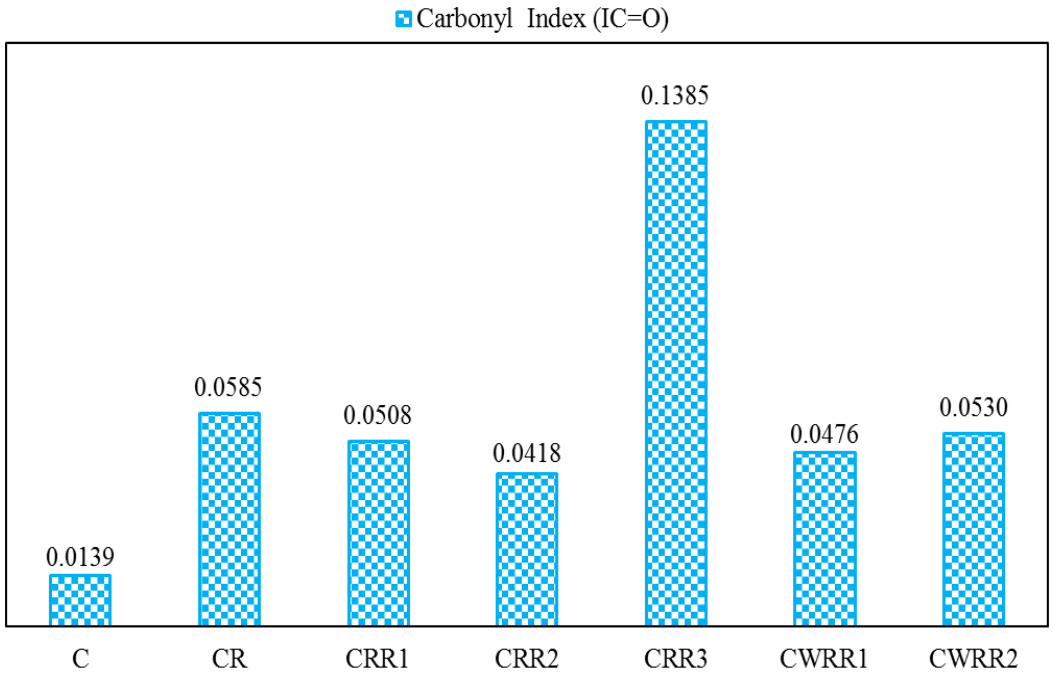

(a)

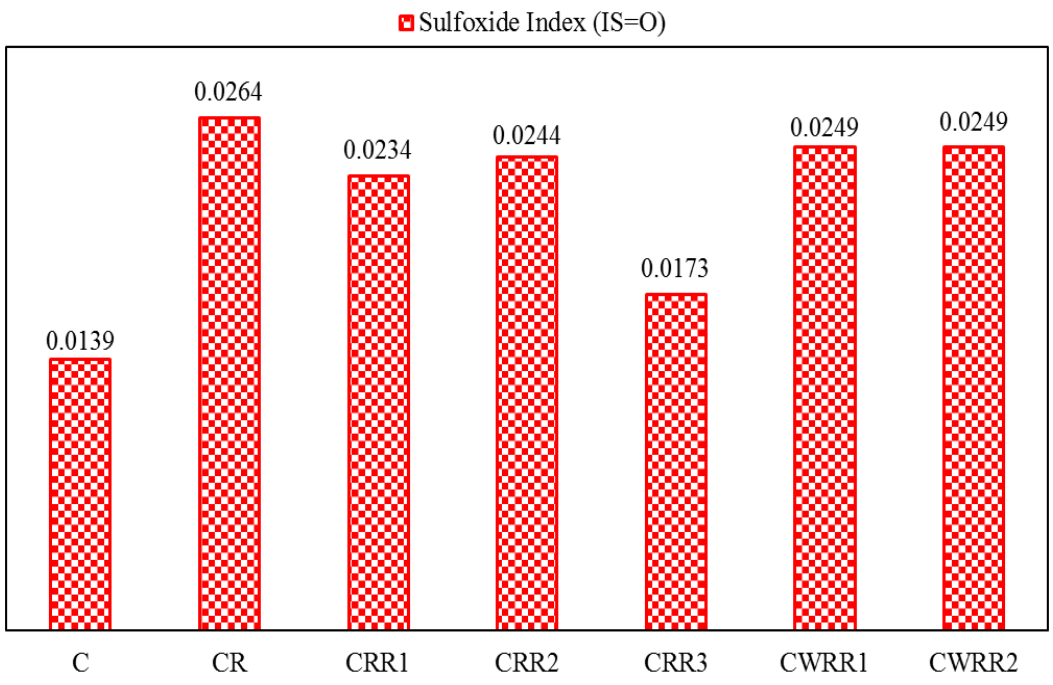
Sulfoxide Index (IS=O)
0.0139
0.0264
0.0234
0.0244
0.0173
0.0249
0.0249
C
CR
CRR1
CRR2
CRR3
CWRR1
CWRR2

(b)

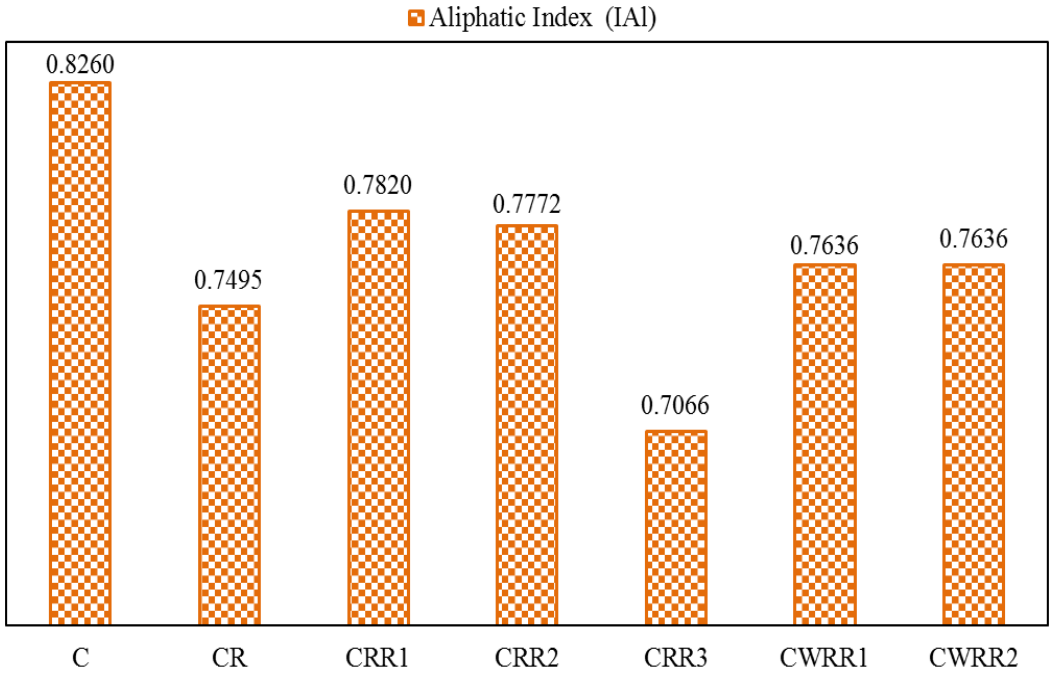
Aliphatic Index (IAl)
0.8260
0.7495
0.7820
0.7772
0.7066
0.7636
0.7636
C
CR
CRR1
CRR2
CRR3
CWRR1
CWRR2

(c)

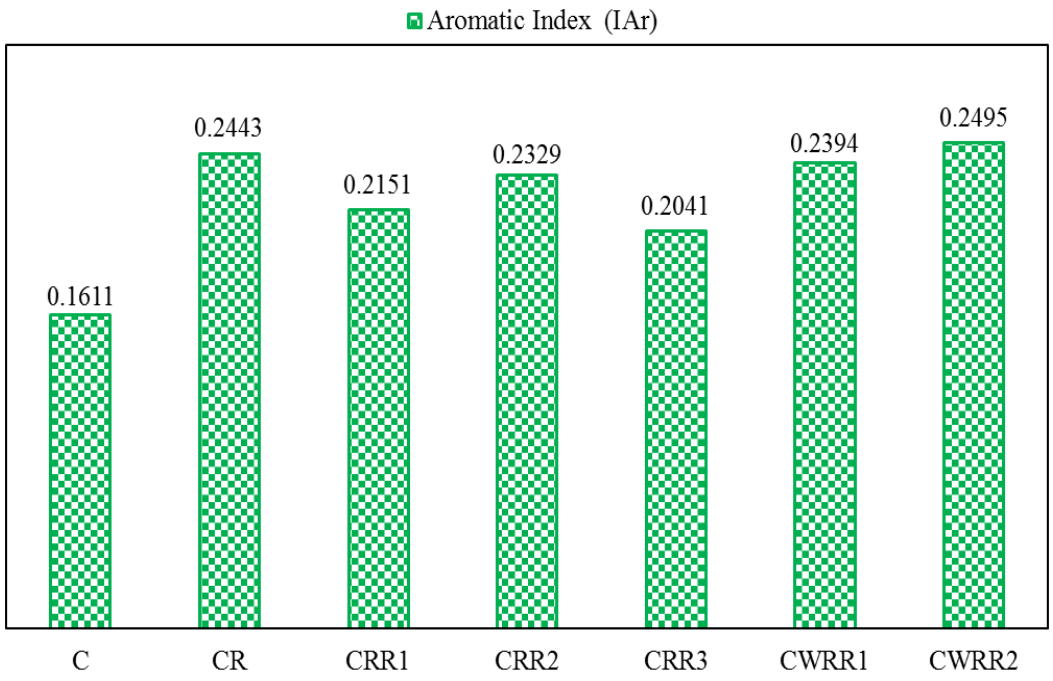

(d)

Figure 4-21. FTIR structural index: (a) carbonyl, (b) sulfoxide, (c) aliphatic, and (d) aromatic.

4.3.4 SARA Tests

Although the analysis of the chemical composition and the structural changes of the binder is very complex, one simple and widely-used approach is to consider the binder as a mixture of saturate, aromatic, resin, and asphaltene (SARA) fractions. The saturate fraction consists of nonpolar linear, branched, and cyclic hydrocarbons, while the aromatics contain one or more polarizable rings. The remaining two fractions, resins and asphaltenes, include polar species. Although resins and asphaltenes have similar structural configurations, the smaller molecular weight of resins (< 1,000 g/mole) leads to their solubility in heptane and pentane, while asphaltenes are somewhat insoluble (Andersen and Speight, 2001; Subirana and Sheu, 2013).

In this study, an IATROSCAN MK-6 was used to find the percentage of each asphalt binder component (i.e., SARA) in different binders. First, the CHROMOROD was cleaned and activated by hydrogen flame through the blank scan IATROSCAN. It should be noted that the CHROMOROD, developed exclusively for the IATROSCAN, is a thin layer consisting of a thin quartz rod sintered with inorganic binder. Approximately 1.0 μl of the sample solution was spotted on the CHROMOROD by means of a micro-dispenser. When the components in the sample were separated, the measurement of SARA fractions was made.

The results of SARA tests for different binders are presented in Figure 4-22. As the figure shows, the SARA analysis of the CR binder (the mixture of control binder C and the recycle asphalt binder (RAB) shows an increase in asphaltenes, resins, and saturates, and a decreases in aromatics. The green-tech rejuvenator (R3) dilutes saturates and substantially dilutes the asphaltenes and the

aromatics of the CR binder but increases the resin. This could be related to the bio source of this rejuvenator. In addition, both the agriculture- and petroleum-tech rejuvenators (R1 and R2) increase the aromatics and decrease the asphaltenes, resins, and saturates.

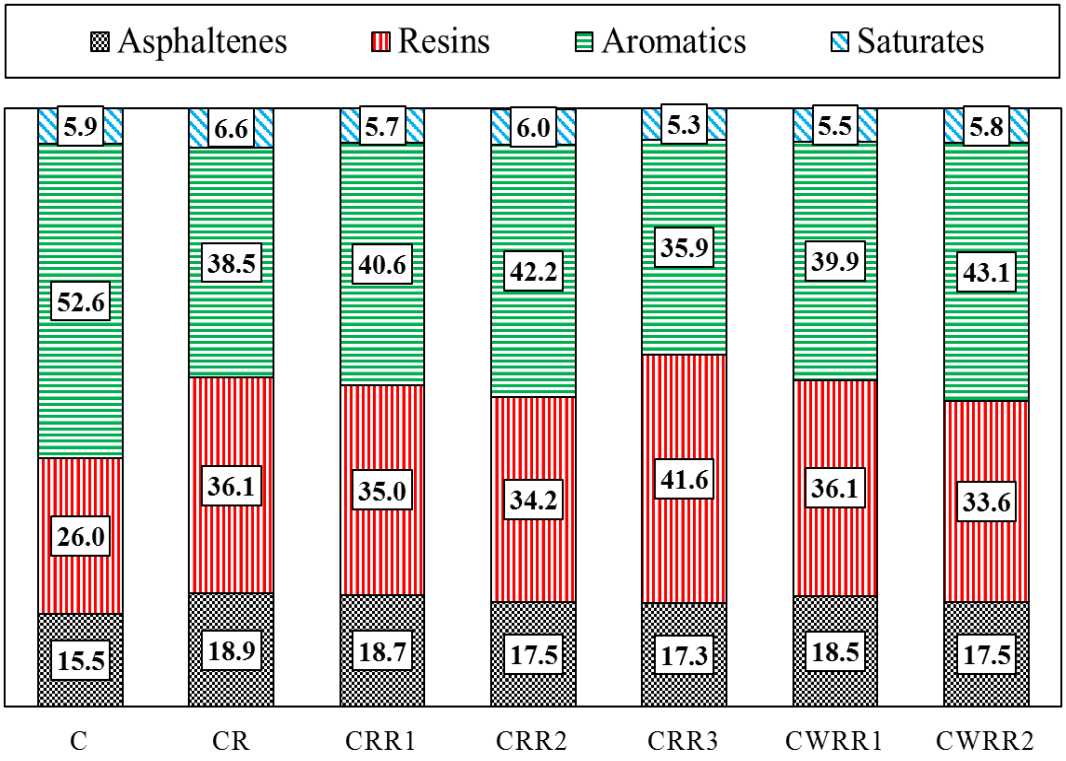

Figure 4-22. Percentage of SARA components (i.e., asphaltenes, resins, aromatics, and saturates) for each binder.

With the SARA analysis results, the colloidal instability index (CII), which is defined as the ratio of "the sum of aromatics and resins" to "the sum of asphaltenes and saturates" (Feng et al., 2012), can be quantified as a screening criterion. The CII is generally used to identify the binder systems with deposit problems. In the aging process, a series of transformations occur due to the presence of oxygen; the aromatics to resins and then the resins to asphaltenes. During this process, the ratio of maltenes to asphaltenes reduces and consequently, lower amounts of maltenes are available for the dispersion of the asphaltenes (NCAT, 2014). This results in higher viscosity, lower ductility, and smaller value of CII. The CII values and the percentage of relative change of each binder to the control binder (C) are presented in Table 4-6. Furthermore, the ratio of maltenes to asphaltenes is shown in Figure 4-23.

Table 4-6. Values of CII and Its Relative Changes.

Binder	CII	Change relative of each binder to the control binder (%)
C	3.67	
CR	2.93	-20%
CRR1	3.10	-16%
CRR2	3.25	-11%
CRR3	3.43	-7%
CWRR1	3.17	-14%
CWRR2	3.29	-10%

According to the results presented in Table 4-6, the blend of RAB with control binder (C), namely CR, has a 20% decrease in CII compared to the C binder. The agriculture-tech rejuvenator (R1) and petroleum-tech rejuvenator (R2) led to a 16% and 11% drop in CII compared to the C, respectively. Also, only a 7% decrease was observed by the addition of green-tech rejuvenator (R3). Moreover, the presence of agriculture-tech rejuvenator (R1) and petroleum-tech rejuvenator (R3) in the binder treated by WMA technology (i.e., CWRR1 and CWRR2) can increase CII values compared to their counterparts (i.e., CRR1 and CRR2).

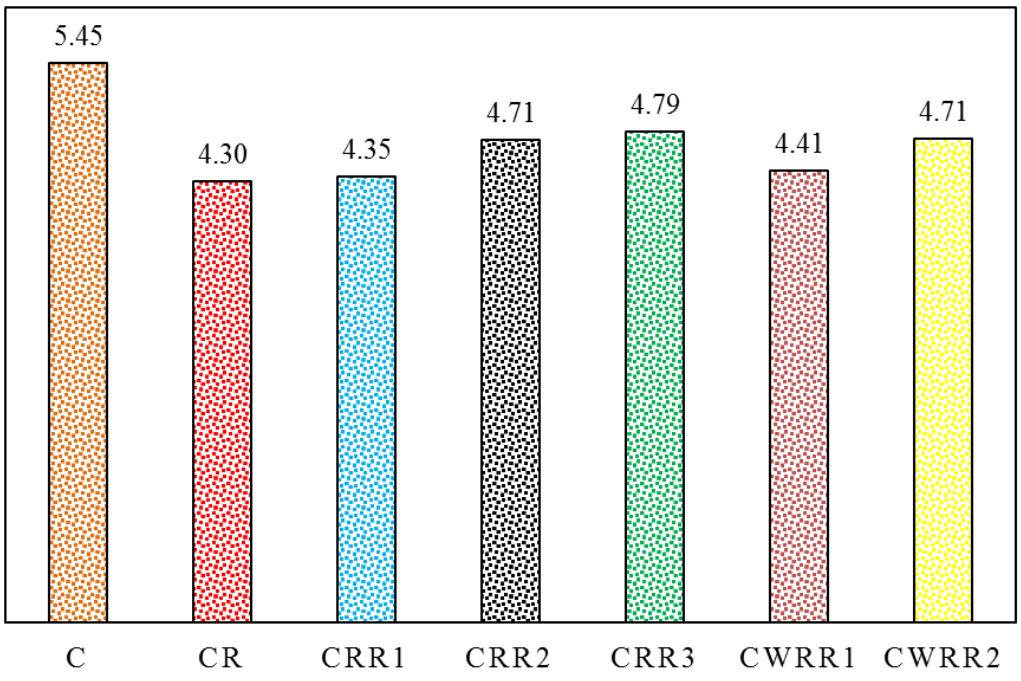

Figure 4-23. Ratio of maltenes to asphaltenes.

As can be seen in Figure 4-23, the ratio of maltenes to asphaltenes in the control binder decreased when the RAB binder was added. It can be clearly observed that adding rejuvenators can increase this ratio, which indicates the capability of the rejuvenators to restore the chemical composition of the CR binder. However, the maltenes to asphaltenes ratio of CR (4.30) and CRR1 (4.35) are similar, and this ratio is 4.71 and 4.79 for the petroleum- and green- tech rejuvenators, respectively. It implies that the effect of petroleum- and green-tech rejuvenators to restore chemical composition of the CR binder is more significant than agriculture-tech rejuvenator.

4.4 Linkage between AC Mixtures and FAM Mixtures

This section explores a linkage between performance characteristics of the AC mixture and its corresponding FAM phase by comparing experimental test data and relevant analysis results through multiple tests.

4.4.1 Stiffness Linkage of AC and FAM

Stiffness characteristic of AC mixture and its corresponding FAM was evaluated by performing frequency sweep tests on both length scales. The frequency sweep test on the AC specimen was performed at three test temperatures: 4 ˚C, 20 ˚C, and 40 ˚C. Using the test results, master curves of dynamic modulus were plotted at 20 ˚C as they are presented in Figure 4-24(a). Also, the results of frequency sweep test on FAM specimens were used to obtain master curves of dynamic shear modulus at 20 ˚C as illustrated in Figure 4-24(b).

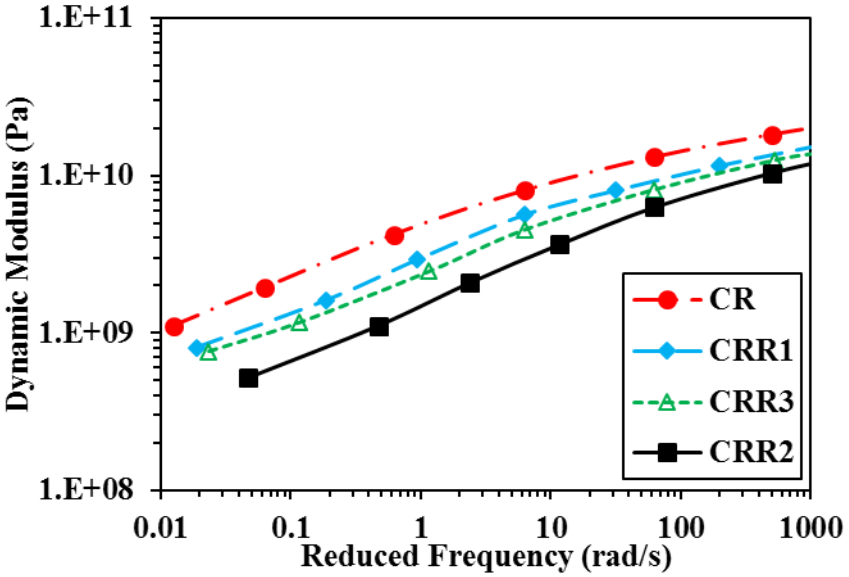

(a)

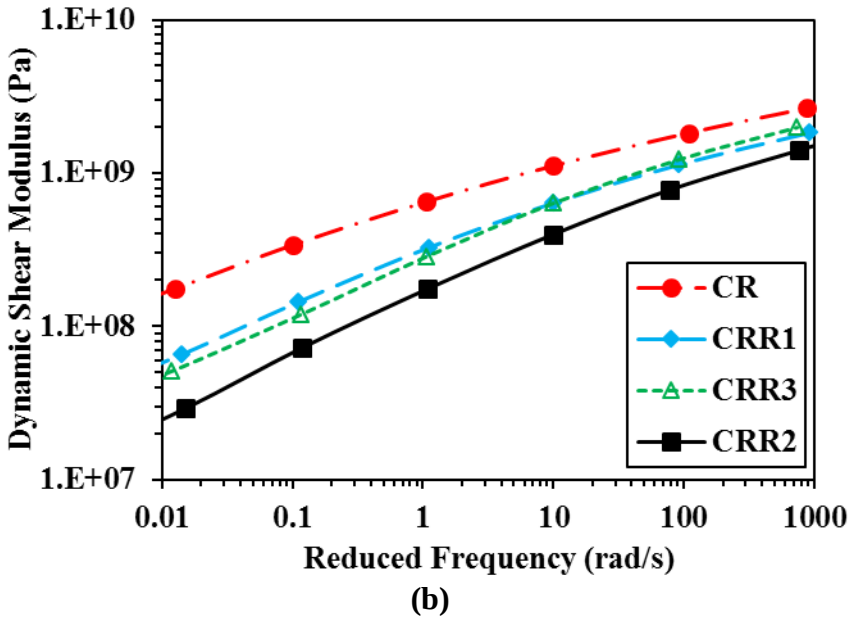

Figure 4-24. Dynamic modulus test results of (a) AC mixtures; (b) FAM mixtures.

The AC mixture test results showed that the petroleum-tech rejuvenated mixture was softest, and the CR mixture was the stiffest. Mixtures containing agriculture-tech and green-tech rejuvenators showed similar behavior. The test results of FAM mixture demonstrated that the CR mixture and the petroleum-tech rejuvenated mixture showed the stiffest and the softest behavior, respectively. The green-tech and the agriculture-tech rejuvenators showed similar softening effects on FAM. Therefore, AC mixture and FAM mixture test results were generally in agreement with each other.

4.4.2 Fatigue Cracking Linkage of AC and FAM

Time sweep test results of FAM mixtures were compared with test results of SCB test of AC mixtures to explore a linkage in cracking behavior between the two length scales. Although both tests targeted mixture failure due to cracking, it should be noted that the time sweep test of FAM specimens was performed using a torsional shearing mechanism, while the SCB test of AC mixture specimens was conducted to induce opening mode cracking and failure.

In order to explore a linkage between the two, a cracking-related indicator of the SCB fracture test was necessary so that it can be compared to the time sweep fatigue test results (such as fatigue life) of FAM mixtures. To this end, four indicators including the flexibility index (FI), the fracture energy, the pre-peak slope (m1), and the post-peak slope (m2) in the SCB load-displacement curve were investigated (Table 4-1). Among the four potential indicators, the FI showed a good correlation with the FAM fatigue test (time sweep test) results (Table 4-7). This implies that the FI in the SCB fracture test represents the mixture's rate of damage, which is particularly related to cracking.

Table 4-7. Comparison between FI (AC) and Fatigue Life (FAM)

Mixture	CR	CRR3	CRR1	CRR2
Strain (%)	**Fatigue Life**			
0.15	117790	221700	299800	304600
0.15	74295	163990	238900	265490
0.15	50992	79189	30889	183190
0.2	60584	32896	68486	112300
0.2	32398	26093	17890	90101
0.2	21099	23893	8785	84792
0.25	11358	15696	17055	33085
0.25	11046	8801	8395	21899
0.25	7035	5856	7689	20805
Ave. Fatigue Life	**42955**	**64235**	**77543**	**124029**
FI	**9.4**	**11.5**	**13.9**	**17.9**

4.4.3 Permanent Deformation Linkage of AC and FAM

Permanent deformation linkage was evaluated by comparing the results of dynamic creep test of AC mixtures and static creep test of FAM mixtures. Dynamic creep tests were performed on the AC cylinders at 40 ˚C with 138 kPa uniaxial pressure. Loading time and rest period were 0.1 and 0.9 seconds. Tests were continued until 10,000 cycles or 100,000 seconds. Test results are presented in Figure 4-25 (a). Dynamic creep AC mixtures were compared with the static creep test results of FAM mixtures at a stress level of 75 kPa. As shown in Figure 4-25, both tests yielded the same rank order of permanent deformation among the four mixtures. As shown and expected, the CR mixture experienced the lowest amount of permanent deformation, while other rejuvenated mixtures presented larger strains due to more compliant mixture characteristics. Although the comparison between the AC and FAM is qualitative, AC rank order generally agrees with FAM rank order. Although further investigations are necessary to reach any definite conclusions, it was observed that there is a strong linkage between the AC mixture and its corresponding FAM phase in the inelastic deformation characteristics. This implies that the AC mixture characteristics can hypothetically be predicted (or estimated) from FAM testing, which would significantly save experimental efforts required to perform AC testing.

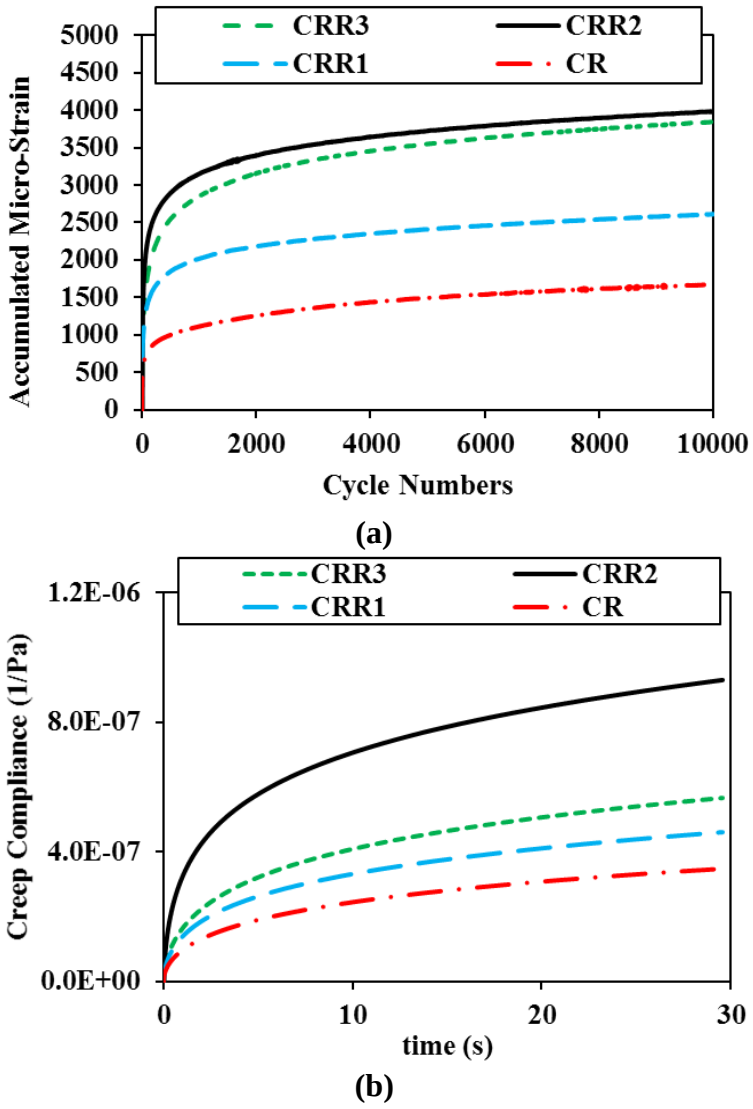

Figure 4-25. Results of (a) dynamic creep tests of AC mixtures and (b) static creep test of FAM mixtures.

Chapter 5 Summary, Conclusions and Recommendations

In this study, three different rejuvenators (petroleum, green, and agriculture) and an amine-based WMA additive were added to the Nebraska asphalt mixture with 65% RAP content. The results of various laboratory tests, including dynamic modulus, dynamic creep, SCB fracture test on AC (under dry and wet conditions), three types of strain-controlled torsional oscillatory shear tests (strain sweep, frequency sweep, and time sweep), and static multiple stress creep-recovery tests on FAM were compared. In addition, four types of binder tests including the DSR, AFM, FTIR, and SARA were carried out. The following conclusion can be made based on the test-analysis results:

- Rejuvenators softened the high-RAP mixtures, which increased the rutting potential of the mixture. The petroleum-tech rejuvenator had the most significant effect on mixture softening, and the agriculture-tech rejuvenator had the lowest effect. The softening effect of rejuvenators in the high-RAP mixture could increase mixture ductility, which helped improve cracking resistance of the RAP mixture.
- Rejuvenators typically compromised moisture damage resistance of the high-RAP mixture. The green-tech rejuvenator used in this study showed the highest detrimental effect than the other two rejuvenators.
- Experimental results of the two length scales (AC vs. FAM) generally showed a good agreement in viscoelastic stiffness characteristics, fatigue cracking potential, and permanent deformation characteristics. This indicates that there is a linkage between the AC and FAM. Although more studies and investigations with many other cases need to be carried out to reach any definite conclusions, FAM scale tests appear to be a good alternative for predicting AC mixture behavior.
- Introducing the agriculture-tech and petroleum-tech rejuvenators (i.e., R1 and R2) to the binder CR resulted in a decrease in the carbonyl, sulfoxide and aromatic indices and an increase in aliphatic index. This indicates that the rejuvenators can restore the chemical compositions of aged binder. The impact of green-tech rejuvenator was quite different from the other two rejuvenators: the carbonyl index increased and aliphatic index decreased, which was in an opposite trend from the binders mixed with the other two rejuvenators.
- The blending of the aged binder with the control virgin binder resulted in a decrease in colloidal instability index (CII). The CII increased by adding rejuvenators to the aged binder. The effect of petroleum-tech and green-tech rejuvenators on restoring the chemical composition of the aged binder was more pronounced than agriculture-tech rejuvenator.
- AFM tests showed that the addition of the rejuvenators to the aged binder changed the "bee-shaped" structure by reducing their size and number. AFM phase images of binders confirmed that the presence of rejuvenators in the CR asphalt binder, results in a darker color of the flat matrix of CR asphalt binder; i.e., the flat matrix of rejuvenated binders is softer than CR.
- The DSR test results showed that the mechanical behavior of binders treated with the rejuvenators is quite different from binders without rejuvenators. Adding the rejuvenator generally softened the aged binder, and the extent of influence is different due to the nature of the rejuvenator. It can be seen that the impact of green-tech rejuvenator on softening of binder is more significant than the petroleum-tech and agriculture-tech rejuvenators.

- The obtained results revealed that dosage rates of rejuvenators affect the binder and mixture properties. The effect of agriculture tech rejuvenator (R1) on chemical and mechanical properties of the binder and mixture was not significant compared to the other rejuvenators, since its dosage rate was much lower than that of the other rejuvenators. On the other hand, the higher dosage rate of the green tech rejuvenator (R3) changed properties of binder and mixture remarkably.

5.1 Recommended Future Research

In this research study, the dosage rates of rejuvenators and their blending procedures were selected and performed based on the manufacturers' recommendation. Although the recommended dosages satisfied volumetric mix design criteria; as a common/routine procedure for selecting proper dosage of rejuvenator, the obtained results show that other dosage rates should have been investigated. For example, the Soybean oil (R1) did not change the properties of the binder or mixture significantly, while the Hydrogreen (R3) effects were very substantial. It is worthy to note that the suggested dosage of Soybean oil and Hydrogreen were 1.6 and 8.2%, respectively, by weight of total binder. In addition, the Soybean oil was added to the hot virgin binder and then blended with the mixture (RAP and virgin aggregate), while Hydrogreen was directly added to the mixture (RAP, virgin aggregate and virgin binder). To more accurately compare the effects of rejuvenators, an optimization study should be carried out. Additionally, different blending procedures of rejuvenators may have a valuable impact on binder and mix design properties. For example, if rejuvenators could solely be designed to be coated or blended on the RAP material prior to introduction into the plant, i.e. pugmilled then stockpile-marinated, RAP drum preheater/precoater etc. Some of these require modifications to existing plants and equipment, but these areas look to show promising results and provide more accurate process control of rejuvenators, by providing direct physical contact with the RAP material which is where all of the rejuvenation needs to be occurring.

This continued research is needed to find the optimum rate of rejuvenators required and study the sequence of blending techniques of the recycled asphalt binder (RAB) and virgin binder as well as the rejuvenator. In addition, a life-cycle cost analysis for the different rejuvenators is needed.

References

AASHTO (2008). "AASHTO TP 62-07 Determining the Dynamic Modulus of Hot Mix Asphalt (HMA) Concrete Mixture." American Association of State and Highway Transportation Officials, Washington, D.C.

AASHTO (2011). "AASHTO TP 79-11 Determining the Dynamic Modulus and Flow Number for Hot Mix Asphalt (HMA) Using the Asphalt Mixture Performance Tester (AMPT)." American Association of State and Highway Transportation Officials, Washington, D.C.

Al-Qadi, I., Lippert, D., Ozer, H., and Thompson, M. (2015). "ICT Engineering for Performance and Sustainability of Future Paving Asphalt Materials." <web: http://ict.illinois.edu/.>.

Al-Qadi, I. L., Aurangzeb, Q., Carpenter, S. H., Pine, W. J., and Trepanier, J. (2012). "Impact of high RAP contents on structural and performance properties of asphalt mixtures." FHWA-ICT-12-002.

Al-Qadi, I. L., Carpenter, S. H., Roberts, G., Ozer, H., Aurangzeb, Q., Elseifi, M., and Trepanier, J. (2009). "Determination of usable residual asphalt binder in RAP." Illinois Center for Transportation (ICT).

Andersen, S. I., and Speight, J. G. (2001). "Petroleum resins: separation, character, and role in petroleum." Petroleum science and technology, 19(1-2), 1-34.

Behnia, B., Ahmed, S., Dave, E. V., and Buttlar, W. G. (2010). "Fracture characterization of asphalt mixtures with reclaimed asphalt pavement." International Journal of Pavement Research and Technology, 3(2), 72-78.

Bonaquist, R. (2013). "Impact of Mix Design on Asphalt Pavement Durability." Enhancing the Durability of Asphalt Pavements, 1.

Boriack, P. C., Katicha, W. S., Flintsch, W. G., Tomlinson, C. R. (2014). "Laboratory Evaluation of Asphalt Concrete Mixtures Containing High Contents of Reclaimed Asphalt Pavement (RAP) and Binder." Virginia Tech Transportation Institute, FHWA/VCTIR 15-R8.

Branco, C. (2009). "A unified method for the analysis of nonlinear viscoelasticity and fatigue cracking of asphalt mixtures using the dynamic mechanical analyzer." Doctoral Dissertation, Texas A&M University.

Carpenter, S. H., and Wolosick, J. R. (1980). "Modifier influence in the characterization of hot-mix recycled material." Transportation Research Record (777), 15-22.

Chowdhury, A., and Button, J. W. (2008). "A review of warm mix asphalt." Texas Transportation Institute, SWUTC/08/473700-00080-1.

Claine Petersen, J. (1998). "A dual, sequential mechanism for the oxidation of petroleum asphalts." Petroleum Science and Technology, 16(9-10), 1023-1059.

Copeland, A. (2011). "Reclaimed asphalt pavement in asphalt mixtures: state of the practice." Office of Infrastructure Research and Development Federal Highway Administration, FHWA-HRT-11-021.

Cross, S. A., Jakatimath, Y., and KC, S. (2007). "Determination of dynamic modulus master curves for Oklahoma HMA mixtures." Oklahoma State University, FHWA/OK 07 (05).

Daniel, J., Pochily, J., and Boisvert, D. (2010). "Can more reclaimed asphalt pavement be added? Study of extracted binder properties from plant-produced mixtures with up to 25% reclaimed asphalt pavement." Transportation Research Record: Journal of the Transportation Research Board (2180), 19-29.

Feng, Z.-g., Bian, H.-j., Li, X.-j., and Yu, J.-y. (2016). "FTIR analysis of UV aging on bitumen and its fractions." Materials and Structures, 49(4), 1381-1389.
Feng, Z., Yu, J., and Liang, Y. (2012). "The relationship between colloidal chemistry and ageing properties of bitumen." Petroleum Science and Technology, 30(14), 1453-1460.
Ferry, J. D. (1980). Viscoelastic properties of polymers, John Wiley & Sons.
Gardiner, M., and Wanger, C. (1999). "Use of RAP in Superpave HMA Applications." Transportation Research Board-TRB (1681), 10-18.
Ghabchi, R., Singh, D., and Zaman, M. (2014). "Evaluation of moisture susceptibility of asphalt mixes containing RAP and different types of aggregates and asphalt binders using the surface free energy method." Construction and Building Materials, 73, 479-489.
Gibson, N., Qi, X., Shenoy, A., Al-Khateeb, G., Kutay, M., Andriescu, A., Stuart, K., Youtcheff, J., and Harman, T. (2011). "Full-Scale Accelerated Performance Testing for Superpave and Structural Validation: Transportation Pooled Fund Study TPF-5 (019) and SPR-2 (174) Accelerated Pavement Testing of Crumb Rubber Modified Asphalt Pavements." Federal Highway Administration, Report No. FHWA-HRT-11-045, McLean, VA.
Glover, C. J., Martin, A. E., Chowdhury, A., Han, R., Prapaitrakul, N., Jin, X., and Lawrence, J. (2009). "Evaluation of binder aging and its influence in aging of hot mix asphalt concrete: literature review and experimental design." FHWA/TX-08/0-6009-1.
Haghshenas, H., Nabizadeh, H., Kim, YR. (2016). " The Effect of Rejuvenators on RAP Mixtures: A Study Based on Multiple Scale Laboratory Test Results". American Society of Civil Engineers (ASCE), 697-707.
Hajj, E., Souliman, M., Alavi, M., and Loría Salazar, L. (2013). "Influence of hydrogreen bioasphalt on viscoelastic properties of reclaimed asphalt mixtures." Transportation Research Record: Journal of the Transportation Research Board (2371), 13-22.
Hajj, E. Y., Sebaaly, P., Loria, L., Said, K., and Kass, T. L. "Impact of High RAP Content on the Performance Characteristics of Asphalt Mixtures in Manitoba." Proc., Innovative Developments in Sustainable Pavements Session of the 2011 Annual Conference of the Transportation Association of Canada.
Hajj, E. Y., Sebaaly, P. E., and Shrestha, R. (2009). "Laboratory evaluation of mixes containing recycled asphalt pavement (RAP)." Road Materials and Pavement Design, 10(3), 495-517.
Hansen, K. R. (2013). "Performance of High RAP Percentage Mixes." Idaho Asphalt Conference Moscow, Idaho.
Hansen, K. R., and Copeland, A. (2014). "Annual Asphalt Pavement Industry Survey on Recycled Materials and Warm-Mix Asphalt Usage: 2009–2013." Information Series 138, National Asphalt Pavement Association (NAPA).
Hill, B., Oldham, D., Behnia, B., Fini, E., Buttlar, W., and Reis, H. (2013). "Low-Temperature Performance Characterization of Biomodified Asphalt Mixtures That Contain Reclaimed Asphalt Pavement." Transportation Research Record: Journal of the Transportation Research Board (2371), 49-57.
Hoppe, E. J., Lane, D. S., Fitch, G. M., and Shetty, S. (2015). "Feasibility of Reclaimed Asphalt Pavement (RAP) Use As Road Base and Subbase Material.", Virginia Center for Transportation Innovation and Research, VCTIR 15-R6.
Huang, B., Shu, X., and Vukosavljevic, D. (2011). "Laboratory investigation of cracking resistance of hot-mix asphalt field mixtures containing screened reclaimed asphalt pavement." Journal of Materials in Civil Engineering, 23(11), 1535-1543.

Hurley, G. C., and Prowell, B. D. (2006). "Evaluation of Evotherm for use in warm mix asphalt." National Center for Asphalt Technology, NCAT Report 06-02.

Im, S. (2012). "Characterization of viscoelastic and fracture properties of asphaltic materials in multiple length scales." Doctoral Dissertation, University of Nebraska.

Im, S., You, T., Ban, H., and Kim, Y.-R. (2015). "Multiscale testing-analysis of asphaltic materials considering viscoelastic and viscoplastic deformation." International Journal of Pavement Engineering, 1-15.

Im, S., and Zhou, F. (2014). "Field Performance of RAS Test Sections and Laboratory Investigation of Impact of Rejuvenators on Engineering Properties of RAP/RAS Mixes." Texas A&M Transportation Institute, FHWA/TX-14/0-6614-3.

Kandhal, P. S., and Mallick, R. B. (1998). "Pavement Recycling Guidlines for State and Local Goverments Participant's Reference Book." National Center for Asphalt Technology, FHWA-SA-98-042.

Karki, P. (2010). "Computational and experimental characterization of bituminous composites based on experimentally determined properties of constituents." Master Dissertation, University of Nebraska.

Karki, P., Kim, Y.-R., and Little, D. N. "Dynamic Modulus Prediction of Asphalt Concrete Mixtures Through Computational Micromechanics." Transportation Research Board (2507), 1-9.

Kavussi, A., Qorbani, M., Khodaii, A., and Haghshenas, H. (2014). "Moisture susceptibility of warm mix asphalt: A statistical analysis of the laboratory testing results." Construction and Building Materials, 52, 511-517.

Khodaii, A., Tehrani, H. K., and Haghshenas, H. (2012). "Hydrated lime effect on moisture susceptibility of warm mix asphalt." Construction and Building Materials, 36, 165-170.

Khosla, N. P., Nair, H., Visintine, B., and Malpass, G. (2012). "Effect of reclaimed asphalt and virgin binder on rheological properties of binder blends." International Journal of Pavement Research and Technology, 5(5), 317.

Kim, Y.-R., and Aragão, F. T. S. (2013). "Microstructure modeling of rate-dependent fracture behavior in bituminous paving mixtures." Finite Elements in Analysis and Design, 63, 23-32.

Kim, Y.-R., Little, D., and Lytton, R. (2002). "Use of dynamic mechanical analysis (DMA) to evaluate the fatigue and healing potential of asphalt binders in sand asphalt mixtures (with discussion and closure)." Journal of the Association of Asphalt Paving Technologists, 71, 176-206.

Kim, Y.-R., Little, D., and Lytton, R. (2003). "Fatigue and healing characterization of asphalt mixtures." Journal of Materials in Civil Engineering, 15(1), 75-83.

Kim, Y.-R., and Little, D. N. (2005). "Development of specification-type tests to assess the impact of fine aggregate and mineral filler on fatigue damage." Texas Transportation Institute, FHWA/TX-05/0-1707-10.

Kim, Y.-R., Little, D. N., and Song, I. (2003). "Mechanistic evaluation of mineral fillers on fatigue resistance and fundamental material characteristics." Transportation Research Board (1832), 1-8.

Kim, Y., Lee, H., Little, D., and Kim, Y. R. (2006). "A Simple Testing Method to Evaluate Fatigue Fracture and Damage Performance of Asphalt Mixtures (With Discussion)." Journal of the Association of Asphalt Paving Technologists, 75, 755-787.

Kim, Y. T. (2011). "Performance Measures of Warm Asphalt Mixtures for Safe and Reliable Freight Transportation Phase II: Evaluation of Friction and Raveling Characteristics of Warm Mix Asphalt Mixtures with Anti-stripping Agents." Public Policy Center, University of Iowa, 25-1121-0001-373.

Kuang, Y. (2012). "Evaluation of Evotherm as a WMA technology compaction and anti-strip additive." Master Dissertation, Iowa State University.

Lamontagne, J., Dumas, P., Mouillet, V., and Kister, J. (2001). "Comparison by Fourier transform infrared (FTIR) spectroscopy of different ageing techniques: application to road bitumens." Fuel, 80(4), 483-488.

Lee, H.-J. (1996). Uniaxial constitutive modeling of asphalt concrete using viscoelasticity and continuum damage theory.

Li, R., Karki, P., Hao, P., and Bhasin, A. (2015). "Rheological and low temperature properties of asphalt composites containing rock asphalts." Construction and Building Materials, 96, 47-54.

Li, X., Clyne, T. R., and Marasteanu, M. O. (2004). "Recycled asphalt pavement (RAP) effects on binder and mixture quality." University of Minnesota, MN/RC – 2005-02.

Li, X., and Gibson, N. "Analysis of RAP with Known Source History and Influence on Fatigue Performance." Transportation Research Board 92nd Annual Meeting, 13-4901.

Li, X., Marasteanu, M., Williams, R., and Clyne, T. (2008). "Effect of reclaimed asphalt pavement (proportion and type) and binder grade on asphalt mixtures." Transportation Research Record (2051), 90-97.

Loeber, L., Muller, G., Morel, J., and Sutton, O. (1998). "Bitumen in colloid science: a chemical, structural and rheological approach." Fuel, 77(13), 1443-1450.

Lu, X., and Isacsson, U. (2002). "Effect of ageing on bitumen chemistry and rheology." Construction and Building Materials, 16(1), 15-22.

Lu, X., Langton, M., Olofsson, P., and Redelius, P. (2005). "Wax morphology in bitumen." Journal of Materials Science, 40(8), 1893-1900.

Marasteanu, M., and Anderson, D. (2000). "Establishing linear viscoelastic conditions for asphalt binders." Transportation Research Board (1728), 1-6.

Masson, J. F., Leblond, V., and Margeson, J. (2006). "Bitumen morphologies by phase-detection atomic force microscopy." Journal of Microscopy, 221(1), 17-29.

McDaniel, R. S., Shah, A., and Huber, G. (2012). "Investigation of Low-and High-Temperature Properties of Plant-Produced RAP Mixtures." North Central Superpave Center, Purdue University, FHWA-HRT-11-058.

McDaniel, R. S., Shah, A., Huber, G. A., and Gallivan, V. (2007). "Investigation of properties of plant-produced RAP mixtures." Transportation Research Board (1998), 103-111.

McDaniel, R. S., Soleymani, H., Anderson, R. M., Turner, P., and Peterson, R. (2000). "Recommended use of reclaimed asphalt pavement in the Superpave mix design method." NCHRP Web document, 30.

Mogawer, W. (2012). "Development of Balanced & Eco-Friendly Thin Lift Asphalt Mixtures Incorporating Sustainable Materials." International Pavement Preservation Confernce, University of Massachusetts Dartmouth.

Mogawer, W., Austerman, A., Mohammad, L., and Kutay, M. E. (2013). "Evaluation of high RAP-WMA asphalt rubber mixtures." Road Materials and Pavement Design, 14(sup2), 129-147.

Mogawer, W., Bennert, T., Daniel, J. S., Bonaquist, R., Austerman, A., and Booshehrian, A. (2012). "Performance characteristics of plant produced high RAP mixtures." Road Materials and Pavement Design, 13(sup1), 183-208.

Mogawer, W. S., Booshehrian, A., Vahidi, S., and Austerman, A. J. (2013). "Evaluating the effect of rejuvenators on the degree of blending and performance of high RAP, RAS, and RAP/RAS mixtures." Road Materials and Pavement Design, 14(sup2), 193-213.

Mouillet, V., Lamontagne, J., Durrieu, F., Planche, J.-P., and Lapalu, L. (2008). "Infrared microscopy investigation of oxidation and phase evolution in bitumen modified with polymers." Fuel, 87(7), 1270-1280.

NCAT (2014). "NCAT Researchers Explore Multiple Uses of Rejuvenators." National Center for Asphalt Technology, Auburn, AL.

NCAT (2015). "Warm-mix and RAP: A Winning Combination." National Center for Asphalt Technology, Auburn, AL.

Palvadi, S., Bhasin, A., and Little, D. (2012). "Method to quantify healing in asphalt composites by continuum damage approach." Transportation Research Board (2296), 86-96.

Petersen, J. C. (2000). "Chemical composition of asphalt as related to asphalt durability." Developments in Petroleum Science, 40, 363-399.

Petersen, J. C., and Glaser, R. (2011). "Asphalt oxidation mechanisms and the role of oxidation products on age hardening revisited." Road Materials and Pavement Design, 12(4), 795-819.

Putman, B. J. (2012). "Investigation Of Warm Mix Asphalt (WMA) Technologies And Increased Percentages Of Reclaimed Asphalt Pavement (RAP) In Asphalt Mixtures." Clemson University, FHWA-SC-12-05.

Reese, R. (1997). "Properties of aged asphalt binder related to asphalt concrete fatigue life." Journal of the Association of Asphalt Paving Technologists (66), 604-632.

Sengoz, B., and Oylumluoglu, J. (2013). "Utilization of recycled asphalt concrete with different warm mix asphalt additives prepared with different penetration grades bitumen." Construction and Building Materials, 45, 173-183.

Shen, J., Amirkhanian, S., and Tang, B. (2007). "Effects of rejuvenator on performance-based properties of rejuvenated asphalt binder and mixtures." Construction and Building Materials, 21(5), 958-964.

Shu, X., Huang, B., and Vukosavljevic, D. (2008). "Laboratory evaluation of fatigue characteristics of recycled asphalt mixture." Construction and Building Materials, 22(7), 1323-1330.

Solaimanian, M., Milander, S., Boz, I., and Stoffels, S. M. (2011). "Development of guidelines for usage of high percent RAP in warm-mix asphalt pavements." Pennsylvania State University, University Park, Pennsylvania Department of Transportation, Federal Highway Administration, FHWA-PA-2011-013-PSU, 32, 2012-2002.

Stimilli, A., Canestrari, F., Teymourpour, P., and Bahia, H. U. (2015). "Low-temperature mechanics of hot recycled mixtures through asphalt thermal cracking analyzer (ATCA)." Construction and Building Materials, 84, 54-65.

Subirana, M., and Sheu, E. Y. (2013). Asphaltenes: fundamentals and applications, Springer Science & Business Media.

Tam, K., Joseph, P., and Lynch, D. (1992). "Five-year experience of low-temperature performance of recycled hot mix." Transportation Research Record (1362), 56-65.

Tran, N. H., Taylor, A., and Willis, R. (2012). "Effect of rejuvenator on performance properties of HMA mixtures with high RAP and RAS contents." Auburn, AL: National Center for Asphalt Technology, NCAT Report 12-05.

Tschoegl, N. W. (2012). The phenomenological theory of linear viscoelastic behavior: an introduction, Springer Science & Business Media.

Underwood, B. S., and Kim, Y. R. (2012). "Microstructural Association Model for Upscaling Prediction of Asphalt Concrete Dynamic Modulus." Journal of Materials in Civil Engineering, 25(9), 1153-1161.

Underwood, B. S., and Kim, Y. R. (2013). "Microstructural investigation of asphalt concrete for performing multiscale experimental studies." International Journal of Pavement Engineering, 14(5), 498-516.

Uzarowsk L, Prilesky H, Berube E, Henderson V, and Rizvi R (2010). "Laboratory Testing of Vancouver HMA Mixes Containing Recycled Asphalt Shingles." Transportation Association of Canada Halifax, Nova Scotia.

Vasconcelos, K. L., Bhasin, A., Little, D. N., and Lytton, R. L. (2010). "Experimental measurement of water diffusion through fine aggregate mixtures." Journal of Materials in Civil Engineering, 23(4), 445-452.

West, R. (2010). "Reclaimed asphalt pavement management: best practices." Auburn, AL: National Center for Asphalt Technology, NCAT Draft Report.

West, R., Michael, J., Turochy, R., and Maghsoodloo, S. "A comparison of virgin and recycled asphalt pavements using long-term pavement performance SPS-5 data." Proc., Transportation research board 90th annual meeting. Washington, DC: Transportation Research Board, Paper.

West, R., Timm, D., Willis, R., Powell, B., Tran, N., Watson, D., Sakhaeifar, M., Brown, R., Robbins, M., and Nordcbeck, A. (2012). "Phase IV NCAT pavement test track findings." National Center for Asphalt Technology, Auburn University, NCAT Report 12-10.

West, R. C., Rada, G. R., Willis, J. R., and Marasteanu, M. O. (2013). "Improved mix design, evaluation, and materials management practices for hot mix asphalt with high reclaimed asphalt pavement content" National Cooperative Highway Research Program, NCHRP Report 752.

Xiao, F., Amirkhanian, S., and Juang, C. H. (2007). "Rutting resistance of rubberized asphalt concrete pavements containing reclaimed asphalt pavement mixtures." Journal of Materials in Civil Engineering, 19(6), 475-483.

Zaumanis, M., Mallick, R., and Frank, R. (2013). "Evaluation of Rejuvenator's Effectiveness with Conventional Mix Testing for 100% Reclaimed Asphalt Pavement Mixtures." Transportation Research Board (2370), 17-25.

Zaumanis, M., Mallick, R. B., Poulikakos, L., and Frank, R. (2014). "Influence of six rejuvenators on the performance properties of Reclaimed Asphalt Pavement (RAP) binder and 100% recycled asphalt mixtures." Construction and Building Materials, 71, 538-550.

Zaumanis, M., and Smirnovs, J. "Analysis of possibilities for use of warm mix asphalt in Latvia." Proc., Proceedings of Civil Engineering. International Scientific Conference, 57-64.

Zhang, H., Wang, H., and Yu, J. (2011). "Effect of aging on morphology of organo-montmorillonite modified bitumen by atomic force microscopy." Journal of Microscopy, 242(1), 37-45.

Zhang, J. (2010). "Effects of warm-mix asphalt additives on asphalt mixture characteristics and pavement performance." Master Dissertation, University of Nebraska.

Zhao, S., Huang, B., Shu, X., Jia, X., and Woods, M. (2012). "Laboratory performance evaluation of warm-mix asphalt containing high percentages of reclaimed asphalt pavement." Transportation Research Record: Journal of the Transportation Research Board (2294), 98-105.

Zhou, F., Estakhri, C., and Scullion, T. (2014). "Literature Review: Performance of RAP/RAS Mixes and New Direction." Texas A&M Transportation Institute, FHWA/TX-13/0-6738-1.

Zhou, F., Hu, S., Das, G., and Scullion, T. (2011). "High RAP mixes design methodology with balanced performance." Texas Transportation Institute, FHWA/TX-11/0-6092-2.